



HAL
open science

Neogene Paleostress and Structural Evolution of Trinidad: Rotation, Strain Partitioning, and Strike-slip Reactivation of an Obliquely Colliding Thrust Belt

Jean-Claude Hippolyte, Paul Mann

► **To cite this version:**

Jean-Claude Hippolyte, Paul Mann. Neogene Paleostress and Structural Evolution of Trinidad: Rotation, Strain Partitioning, and Strike-slip Reactivation of an Obliquely Colliding Thrust Belt. C. Bartolini. AAPG Memoir 123: South America–Caribbean–Central Atlantic plate boundary: Tectonic evolution, basin architecture, and petroleum systems: Tectonic evolution, basin architecture, and petroleum systems, C. Bartolini, ed., 123, The American Association of Petroleum Geologists, pp.317 - 346, 2021, AAPG Memoir, 10.1306/13692249m1233851 . hal-03663812

HAL Id: hal-03663812

<https://hal.science/hal-03663812v1>

Submitted on 10 May 2022

HAL is a multi-disciplinary open access archive for the deposit and dissemination of scientific research documents, whether they are published or not. The documents may come from teaching and research institutions in France or abroad, or from public or private research centers.

L'archive ouverte pluridisciplinaire **HAL**, est destinée au dépôt et à la diffusion de documents scientifiques de niveau recherche, publiés ou non, émanant des établissements d'enseignement et de recherche français ou étrangers, des laboratoires publics ou privés.

Accepted Manuscript of :

Hippolyte, J.-C., and P. Mann, 2021, Neogene paleostress and structural evolution of Trinidad: Rotation, strain partitioning, and strike-slip reactivation of an obliquely colliding thrust belt, in C. Bartolini, ed., South America–Caribbean–Central Atlantic plate boundary: Tectonic evolution, basin architecture, and petroleum systems: Tectonic evolution, basin architecture, and petroleum systems: AAPG Memoir 123, p. 317–346. DOI: 10.1306/13692249M1233851

https://archives.datapages.com/data/specpubs/memoir123/data/317_aapg-sp2130317.htm

Neogene Paleostress and Structural Evolution Of Trinidad: Rotation, Strain Partitioning, and Strike-Slip Reactivation of an Obliquely Colliding Thrust Belt

Jean-Claude Hippolyte

Aix Marseille University, CNRS, IRD, INRA, Coll France, CEREGE, Aix-en-Provence, France (e-mail: hippolyte@cerege.fr)

Paul Mann

Department of Earth and Atmospheric Sciences, University of Houston, Houston, Texas 77204 (e-mail: pmann@Central.uh.edu)

ABSTRACT

Kinematic analysis of faults in Trinidad reveal three main stages of the tectonic evolution of the southeastern Caribbean–South American plate boundary. During Stage 1, folds and thrusts identified on seismic lines and capped by a middle Miocene angular unconformity formed. They have been related by previous workers to the initial, oblique collision of the Great Arc of the Caribbean with the passive margin of South America. We propose that middle Miocene east-northeast-trending compression identified in this study initially had a more northwest–southeast direction and has been rotated in a clockwise direction during this collision. This tectonic stage may have resulted in clockwise rotation of structures along the southeastern Caribbean plate margin within a broad, right-lateral, strike-slip zone. During Stage 2 in the late Miocene and middle Pliocene, south-southeast-trending contraction uplifted the Central Range, formed the prominent south-vergent thrusts, bounded by oblique ramps such as the Los Bajos right-lateral strike-slip fault and formed piggy-back basins. This north-northwest–south-southeast trend of compression is compatible with coeval right-lateral shear on the El Pilar fault zone in Trinidad. We interpret this pattern of thrusts and strike-slip faults as the result of strain partitioning. In Stage 3 during the late Pliocene–Quaternary, east-southeast-trending compression reactivated previous thrusts with strike-slip motion, such as the Central Range fault. It deactivated previous, east–west-trending, strike-slip faults such as the El Pilar extension into Trinidad. The polyphase evolution of Trinidad results from the eastward motion of the Caribbean arc and the propagation of the southern Subduction-Transform Edge Propagator (STEP) fault of the Caribbean subduction.

I- INTRODUCTION AND OBJECTIVES

The evolution of arcuate subduction zones is of major interest in geology. The island of Trinidad is located at the southeastern edge of the Caribbean arc. It is located in a key geodynamic position at the transition from oceanic subduction near Barbados to the strike-slip southern margin of the Caribbean plate. The eastward motion of the Caribbean plate has been constrained by its position between two major continental plates, the North and South American plates. Furthermore, the Caribbean plate is bounded by two active subduction zones, in the Lesser Antilles (to the east) and in Central America (to the west).

The US Navy geodetic satellite (GEOSAT) marine gravity data compiled by Sandwell and Smith (2009) show elongate submarine and subaerial belts that can be traced as continuous features from the front of the north–south-trending Lesser Antilles subduction zone and Barbados accretionary prism to the east–west-trending southern edge of the plate in northern South America (Figure 1). Within the north–south-trending Lesser Antilles subduction complex, prominent elongate belts shown on the gravity map in Figure 1 include (1) the Aves ridge, the oldest part of the Cretaceous Great Arc of the Caribbean; (2) the Grenada back-arc basin formed in early Cenozoic time as the modern Lesser Antilles arc migrated eastward and rifted away from the Aves Ridge, leaving it as an inactive, remnant arc (Aitken et al., 2011); (3) the Tobago forearc basin and Tobago–Barbados Ridge (Gomez et al., 2018); and (4) the Barbados accretionary prism, which widens to the south, in part owing to the influx of sediment from the Orinoco delta of eastern Venezuela (Deville et al., 2015; Alvarez et al., 2019).

GPS studies have shown that the present-day Caribbean plate—mainly composed of Cretaceous–Paleogene, oceanic, oceanic plateau, and intraoceanic volcanic arc rocks—moves approximately 20 mm/yr relative to the east relative to South America along east–west-striking, right-lateral, strike-slip faults such as the El Pilar fault zone in Venezuela (Pérez et al., 2001; Weber et al., 2001a; Jouanne et al., 2011; Reinoza et al., 2015; Symithe et al., 2015; Figure 1). Most authors also agree that the present-day position of the Caribbean plate is the culmination of 80 Ma of eastward motion from its area of origin in the eastern Pacific Ocean to its present position, as shown in Figure 1 by the successive positions of the leading edge of the plate (Burke, 1988; Mann et al., 1990; Pindell and Barrett, 1990). Geologic studies in Venezuela and Trinidad have supported the west-to-east Caribbean plate path by showing that a rapid pulse of subsidence at the leading edge of the plate closely tracks the progress of the frontal edge of the plate (the Great Arc of the Caribbean) as the frontal edge of the Caribbean plate obliquely and progressively collides with the passive margin of northern South America (Speed, 1985; Escalona and Mann, 2011; Figure 1). Escalona and Mann (2011) have noted that several of these north–south-trending basement features seen on the gravity map in Figure 1 can be traced as continuous features through a 90° bend centered on the island of Trinidad. The westward continuations of the features can be traced as east–west-trending gravity highs for hundreds of kilometers (tens to hundreds of miles) along the northern margin of South America within a right-lateral, strike-slip, and oblique subduction environment.

The objective of this chapter is to use fault kinematic data from mesoscale faults exposed in outcrops of Miocene and younger rocks in Trinidad to reconstruct the evolution of the paleostress field of Trinidad during the eastward movement of the Caribbean plate. Prior to this study, fault slip data had never been collected in Trinidad. Our first objective was to constrain the kinematics of the main structures and their timing to infer the geodynamic evolution of this segment of plate boundary from Miocene to present. The offshore areas around Trinidad include several basins characterized by compressional and extensional structures (e.g., Payne, 1991; Babb and Mann,

1999; Escalona and Mann, 2011; Garciacaro et al., 2011; Soto et al., 2011; Alvarez et al., 2019). Trinidad allows an onshore study of many of these structures and is of significance as an area rich in petroleum.

Our data then may provide new constraints for explaining the nearly 90° bend of the structures along the strongly curved southeastern margin of the Caribbean plate and the tectonic rotation about vertical axes suggested by paleomagnetic data from northern Venezuela and Tobago (Skerlec and Hargraves, 1980; Burmester et al., 1996). We test two hypotheses using fault kinematic data from Trinidad: (1) the 90° bend at Trinidad is an original bend that is reflective of the original shape of the Caribbean plate as it entered into the area between North and South America. This hypothesis predicts simple paleostress evolution without large-scale rotations (the direction of paleostresses would have remained relatively uniform during the plate insertion process) and (2) large-scale rotations have occurred that have progressively rotated the southern part of the originally north-south-trending Lesser Antilles subduction system, and “plated” it into an east-west orientation along the northern margin of South America. This hypothesis was originally proposed by Skerlec and Hargraves (1980) based on their observations of large, 90° rotations on rocks in northern Venezuela

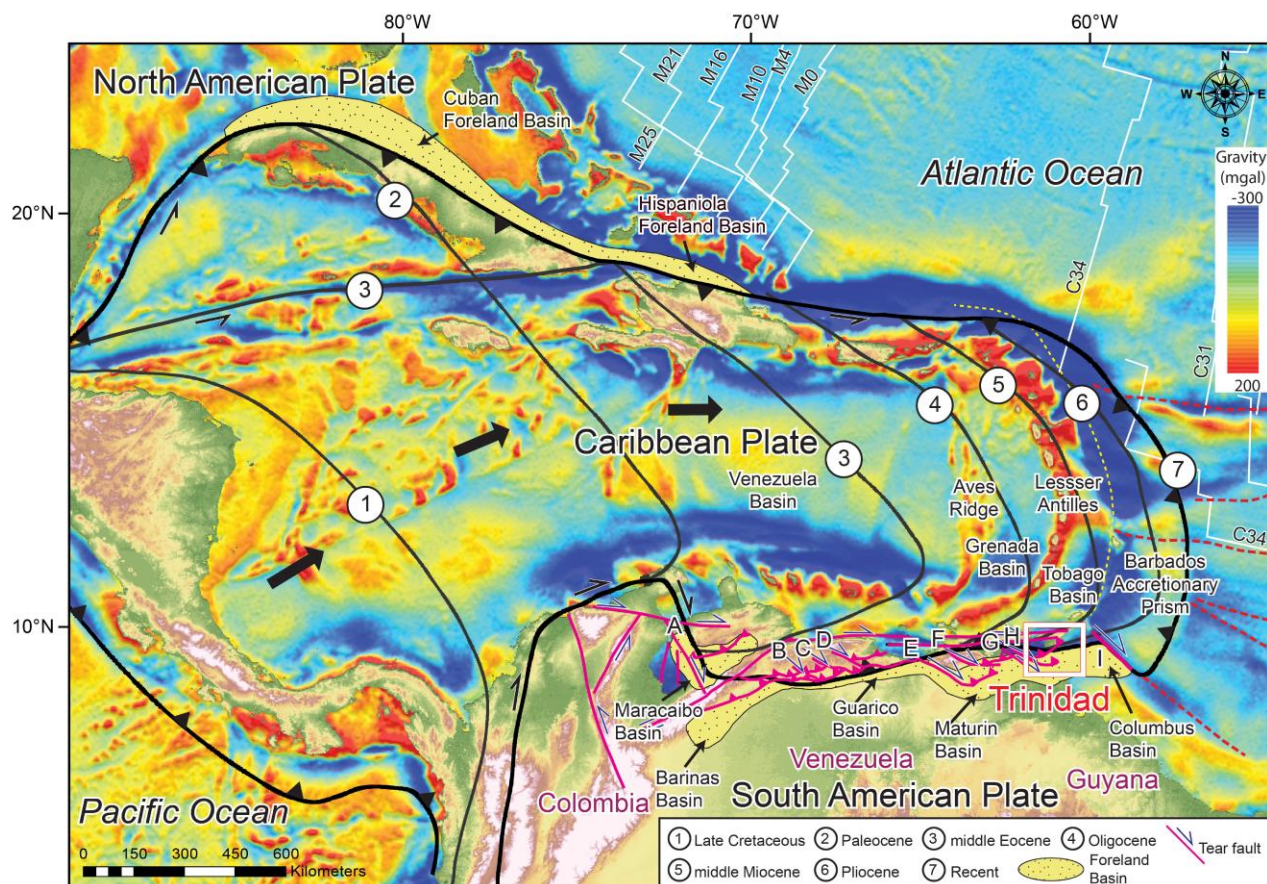


Figure 1. Satellite, free-air gravity map (Sandwell and Smith, 2009) showing geographic features and tectonic provinces of the greater Caribbean and northern South American area modified from Alvarez et al. (2019). The successive positions of the leading edge of the Great Arc of the Caribbean are modified from Escalona and Mann (2011). Numbers refer to the ages shown in the insert. Major plate boundary faults are illustrated by bold black lines. Dashed red lines are fracture zones in Mesozoic to Recent oceanic crust of the Atlantic Ocean. Key: A = Burro Negro tear fault; B, C, and D = Cordillera de la Costa tear faults; E = Urica tear fault; F = San Francisco tear fault; G = El Soldado tear fault; H = Los Bajos tear fault; I = Galera tear fault.

II- STRUCTURAL AND STRATIGRAPHIC SETTING OF TRINIDAD

II-1- Structure

The major structural elements of Trinidad include the structurally uplifted areas of older Cretaceous and Paleogene rocks of the Northern, Central, and Southern ranges as seen on the geologic map of Figure 2 (De Verteuil et al., 2006). Basins between these ranges are filled by upper Miocene sedimentary rocks to Quaternary alluvium (in orange and yellow) and form the Northern and Southern basins.

The highest maximum altitude of about 900 m (3000 ft) is found in the Northern Range, which consists of ductilely deformed metamorphic rocks originally deposited as sediments along the Cretaceous South America passive margin (Frey et al., 1988; Weber et al., 2001b). Lower elevations are found in the Central (~300 m [1000 ft]) and Southern Ranges (~200 m [650 ft]).

The Central Range of Trinidad is a northeast-trending structural uplift with a central core composed of pre-middle Miocene rocks (in green in Figure 2) and flanked by tilted strata as young as Pleistocene. It has been considered to be a south-verging fold-thrust belt (Kugler, 1959; Persad, 1984; Speed, 1985) or a transpressional uplift bounded by inwardly dipping reverse faults, bisected by younger structures of the Central Range strike-slip fault system (Robertson and Burke, 1989; Payne, 1991; Babb and Mann, 1999; Weber et al., 2001a; Giorgis et al., 2009; Soto et al., 2011). In the Northern and Southern basins, tilted and deformed upper Miocene units are inferred to onlap the even more tightly folded and faulted rocks of Oligocene to middle Miocene age, which are exposed at surface in the Central Range.

Seismic data from Trinidad and surrounding offshore areas show that a middle Miocene angular unconformity, outlined in white on the geologic map of Figure 2, is regional in scale and, therefore, both of tectonic importance and of significance for oil exploration (Soto et al., 2011; Alvarez et al., 2019). Folds and thrusts identified on seismic lines are capped by this angular unconformity, which has a short-lived stratigraphic hiatus during the middle Miocene. However, there have been no previous fault kinematic studies to document any stress changes above and below this unconformity.

According to Babb and Mann (1999), other important, tectonic events in the plate boundary evolution of Trinidad that may have affected regional stress and fault history of the island included Pliocene opening of the Gulf of Paria pull-apart basin and Pliocene cessation of strike-slip faulting on the El Pilar fault zone in northern Trinidad (Figure 2). GPS data indicate that the Central Range fault is taking up 12–15 mm/yr of the approximately 20 mm/yr total plate motion (Weber et al., 2001a). Active plate motion is eastward, yet the folds in Trinidad trend east to east-northeast (Figure 2). That most of the folds trend parallel to the GPS vectors suggests that they are not active. Moreover, it suggests that during earlier periods shortening was more north-south in orientation to create east-northeast-trending folds, but no tectonic analyses have yet showed this evolution.

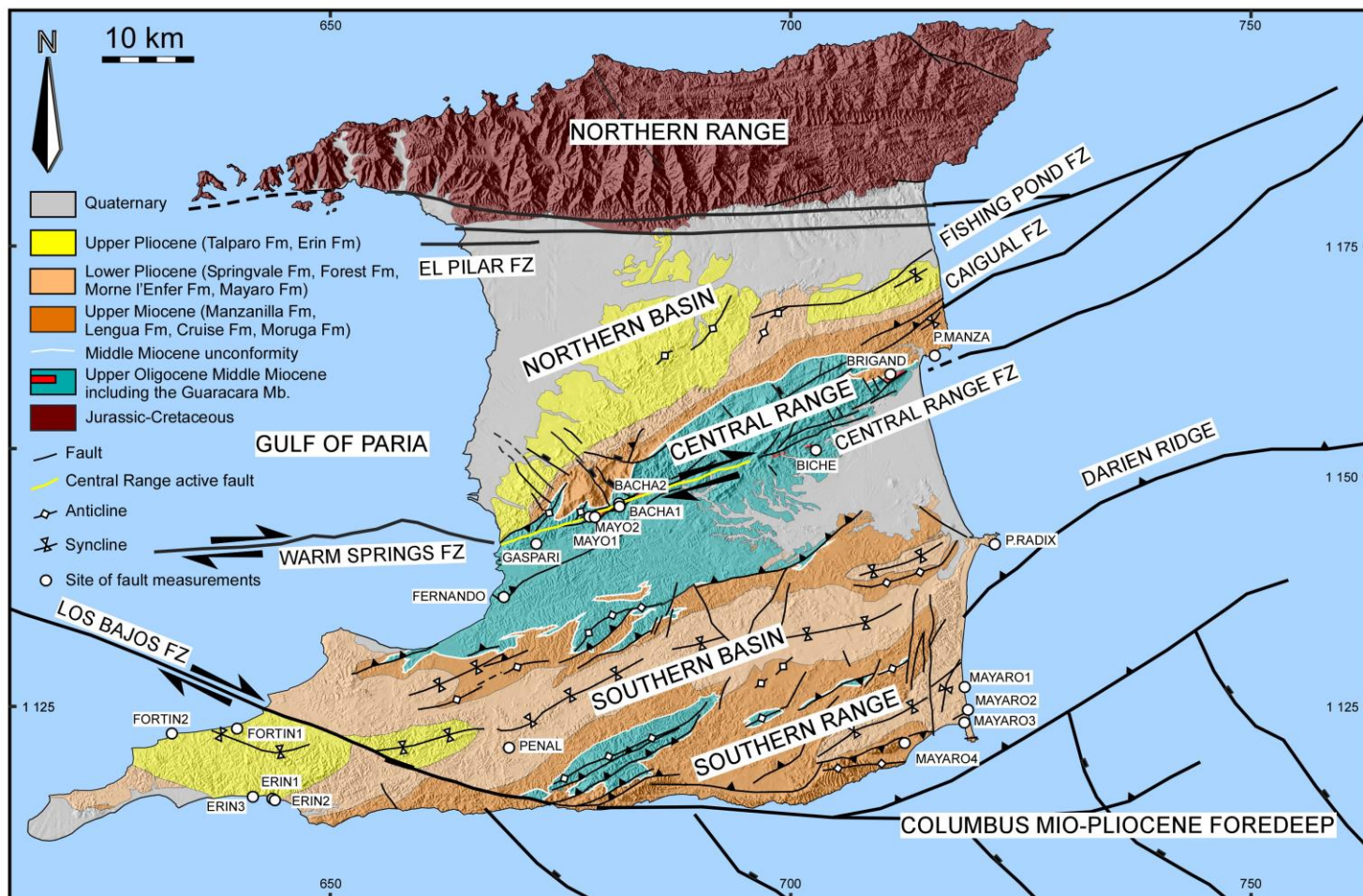


Figure 2. Geological map of Trinidad modified from earlier geologic maps of Trinidad compiled by Kugler (1959) and De Verteuil et al. (2006). The geologic map is superimposed on a shaded topographic basemap. The middle Miocene unconformity is shown as a white line with more highly folded and faulted subunconformity rocks of Mesozoic to Oligocene age shown in blue color. Lighter-colored areas are middle Miocene to recent sedimentary rocks that overlie the middle Miocene unconformity. The 20 sites of microtectonic data collected from outcrops of mesoscale faults are shown as white dots labeled by the abbreviated name of the site, which we refer to in the text. Projection and coordinates for the map are WGS84, UTM Zone 20.

II-2- Stratigraphy

Upper Jurassic–lower Valanginian carbonate rocks are locally exposed in San Fernando (site Fernando in Figure 2), but most of the sedimentary rocks exposed in Trinidad are siliciclastic rocks of Cenozoic age. In the Northern Basin and Central Range of Trinidad, the Brasso Formation consists of mud, shale, and silt of early to middle Miocene age (Wilson, 2007; Figure 3). The Brasso Formation is correlative with the upper part of the Cipero Formation of southern Trinidad (Bolli et al., 1995; Figure 3).

The Brasso Formation includes the Guaracara (Tamana) limestone that is well exposed in quarries in the Central Range (e.g., Erlich et al., 1993). The age of the Guaracara Limestone Member is of particular interest for our fault study because this formation experienced brittle deformation and preserved abundant mesofaults.

Whereas Kugler (2001) proposed that the Tamana Formation overlies the Brasso Formation and is composed by four successive members (the Lower Concord Silt Member, the laterally discontinuous bioherms of the Guaracara Limestone Member, the Upper Concord Silt Member, and the Los Atajos Conglomerate Member; Figure 3), Soto et al. (2011) restricted the name Tamana Formation to the limestone bioherms of central Trinidad. The Lower and Upper Concord Members are lithologically indistinguishable from the Brasso clays, and Wilson (2012) suggested that these names were suppressed and that all of these lithostratigraphic units refer to the Brasso Formation.

Further biostratigraphic work showed that most of the rocks that Kugler (2001) placed in the Tamana Formation are lateral equivalent of the middle Brasso Formation (Erlich et al., 1993; Wilson et al., 2010, 2011; Wilson, 2012). Rocks of the Lower Concord Silt Member, previously thought to be deposited during the late Miocene, were recently dated as late early to early middle Miocene (N6–N10 zones; Figure 3; Wilson, 2012).

The Guaracara Limestone Member crops out discontinuously along the Central Range. Based on lithotypes and fossils, these discontinuous outcrops were interpreted to be limestone bioherms by Erlich et al. (1993) and were named from west to east as the Concord, Gasparillo, Guaracara (Mayo limestone of Wilson, 2012), Tabaquite, Tamana, Biche, and Brigand Hill limestones. Based on foraminiferal abundance biozones, the Guaracara Limestone Member is interpreted as deposited at shallow- to mid-neritic paleodepths (~20–55 m [65–180 ft]) during a series of transgressions and regressions (Wilson et al., 2010).

Erlich et al. (1993) suggested that the age of this member is mainly middle Miocene (Zones N8–N12), whereas Kugler (2001) suggested a late Miocene age (Zones 14–16; Figure 3). Wilson et al. (2010) showed that the Guaracara Limestone Member was largely deposited during the *Globorotalia fohsi fohsi* Zone N10 (Serravalian) and that it is at least partially coeval with the Upper Concord Member of zones N8–N10 (Figure 3; Wilson et al., 2011). Similarly, at Brigand Hill, Wharton et al. (1986) demonstrated that at least part of the limestone was deposited during the Zone 10 in the early middle Miocene (Figure 3).

According to Wilson (2007) and Wilson et al. (2017), the Brasso Formation has been deposited during two tectonically induced Miocene transgressive regressive cycles. These could be related to the eastward advancement of the front of the Caribbean plate (Christenson et al., 2008; Garcacaro et al., 2011). The first cycle ended during the early middle Miocene (N10 Zone) and is locally marked by the development of the Guaracara Limestone (Wilson et al., 2010). At Mayo Quarry, the N9 Zone age was found for Brasso clays immediately underlying the Guaracara Limestone Member (Wilson et al., 2017; Figure 3). The second regressive cycle ranges from the Zone N11 Zone through the N14 Zone (Wilson et al., 2017; Figure 3). The siltstone in the Los Atajos Conglomerate Member and the uppermost claystones of the Brasso Formation are of middle Miocene age (*Globorotalia mayeri* Zone, N14) and cap the shallowing-upward succession (Wilson et al., 2017).

Soto et al. (2011) described 2-D and 3-D seismic reflection data from the eastern shelf off Trinidad to show that the Brasso Formation is separated from the overlying Manzanilla Formation by a pronounced unconformity with its hiatus during the latter part of the middle Miocene. The Los Atajos Member being the uppermost member of the Brasso Formation, Wilson et al. (2017) proposed that the middle Miocene unconformity sensu Soto et al. (2011) encompasses the *Globorotalia menardii* Zone (N15; Figure 3).

The upper Miocene Manzanilla Formation is regarded as marking the deflection toward Trinidad of the palaeo-Orinoco River (Díaz de Gamero, 1996). It commences with the San José

Calcareous Silt Member, deposition of which began during the late Miocene (Zone N16; Figure 3; Wilson, 2013). The marked differences in foraminiferal assemblages between the Los Atajos Member and the overlying Manzanilla Formation support the conclusion that this last member of the Brasso Formation was deposited prior to the late Miocene diversion of the palaeo-Orinoco River toward Trinidad.

In the Northern Basin, upper Miocene–lower Pliocene shallow marine to brackish-water conglomerate and sandstone represent a southward-fining siliciclastic wedge partly derived from the late Miocene uplift and erosion of Trinidad’s Northern Range (Babb and Mann, 1999). Considering that a fault in a transpressional mode can produce high uplifts adjacent to deep basins, these authors proposed that this siliciclastic wedge represents early motion along the El Pilar fault (Figure 2). Lower to middle Pliocene shallow marine and upper Pliocene to Pleistocene marine to brackish-water sand, silt, and clay represent siliciclastic deposition within an increasingly restricted basin between the structurally uplifted Northern Range and Central Range (Babb and Mann, 1999).

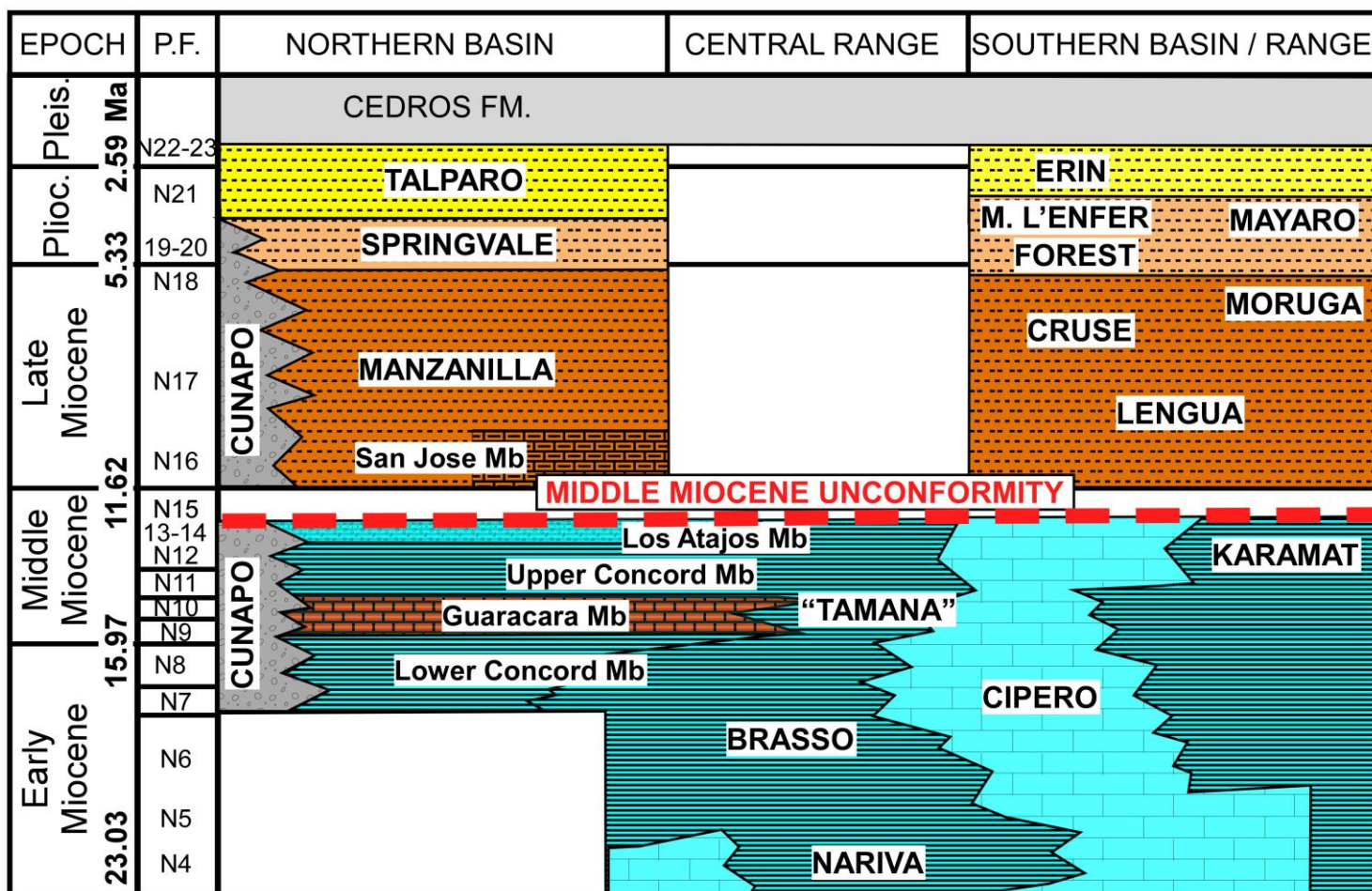


Figure 3. Neogene–Quaternary chronostratigraphic chart of Trinidad of the Northern Range, Central Range, and Southern Basin-Range modified from Erlich et al. (1993), Soto et al. (2011), Wilson (2012), and Wilson et al. (2017).

II-3- Structures and Age of Deformation

Geologic maps of Trinidad show large folds with east-northeast trends, prominently south-vergent thrusts, and long strike-slip faults (Figure 2; Kugler, 1959; Saunders, 1998; and De Verteuil et al., 2006). The Los Bajos and Central Range fault zones strike southeast and east-northeast, respectively, and are oblique to the trend of the El Pilar fault zone like much of the tear faults along the South Caribbean margin (Figures 1, 2). The Los Bajos fault zone shows a possible right-lateral offset by 10.5 km (6.2 mi) of the axis of the Erin-Siparia syncline in the Southern Basin (Wilson, 1940). The syncline is asymmetrical on both sides of the fault, and the southern limb of the syncline is offset by only 6–7 km (3.7–4.3 mi; Figure 2). The Los Bajos fault curves to the northeast along the Southern Range where strike-slip motion may change to thrusting (Figure 2).

The Central Range is cut by range-parallel, right-lateral–strike-slip faults of Pliocene–Pleistocene age (Erlich et al., 1993; Figure 2). A Main Central Range fault was mapped in central Trinidad by Kugler (1953) as a northwest-dipping thrust fault. Babb and Mann (1999) later proposed that the Central Range fault is a subvertical strike-slip fault zone and the onshore continuation of the Warm Springs fault zone in the Gulf of Paria (Figure 2). Weber et al. (2001a, 2011) and Prentice et al. (2010) used GPS, geomorphology, and paleoseismology to map the location of the active modern Central Range fault and measure its rate of slip (Figure 2). Whereas the offshore east–west-trending Warm Springs fault zone appears to have a component of transtension, the onshore Central Range fault zone may have a slight component of transpression (Babb and Mann, 1999; Giorgis et al., 2011).

An interesting aspect of Trinidad's geology is that motion today between the Caribbean and South American plates takes place along east-northeast-strike-slip faults such as the Central Range fault (Figure 2). GPS studies have shown that the Central Range accounts for 12–15 mm/yr of the total plate motion (~20 mm/yr; Weber et al., 2001a). The absence of large historical strike-slip events in the Trinidad area is consistent with the interpretation that the El Pilar fault zone of northern Trinidad area has become inactive (Pérez and Aggarwal, 1981; Speed, 1985; Russo and Speed, 1992; and Babb and Mann, 1999; Figure 2). GPS data show no modern strain accumulation on this fault strand (Weber et al., 2011). The locus of strike-slip motion may thus have changed from that on El Pilar extension along the southern foot of the Northern Range during the late Miocene to the obliquely oriented, Central Range fault in the present day (Babb and Mann, 1999; Weber et al., 2001a).

The middle Miocene angular unconformity separates lower tightly folded and thrustured rocks from less deformed overlying upper Miocene to Quaternary rocks (Figures 2, 3). Rocks below the unconformity are highly deformed because of intense folding and thrusting. Rocks above the unconformity are locally deformed by strike-slip faults and thrusts, in particular in the Southern Basin and Southern Range (Figure 4).

Babb and Mann (1999) recognized a middle Miocene thrusting event that affected the Southern basin and may be related to the late middle Miocene uplift of the Central Range (Figure 2). Following this thrusting event, Babb and Mann (1999) distinguished three Neogene deformation phases that closely control the sequence stratigraphic boundaries: (1) late Miocene–early Pliocene strike-slip motion along the El Pilar fault and north-to-south filling of the Gulf of Paria and Northern basins; (2) middle–late Pliocene strike-slip motion along the Warm Springs–Central Range fault zone and south-to-north filling of the Gulf of Paria and Northern basins; and (3) late Pliocene–Pleistocene strike-slip motion along the Warm Springs–Central Range fault zone and continued filling of the Gulf of Paria and Northern basins. We build on this work in our present study.

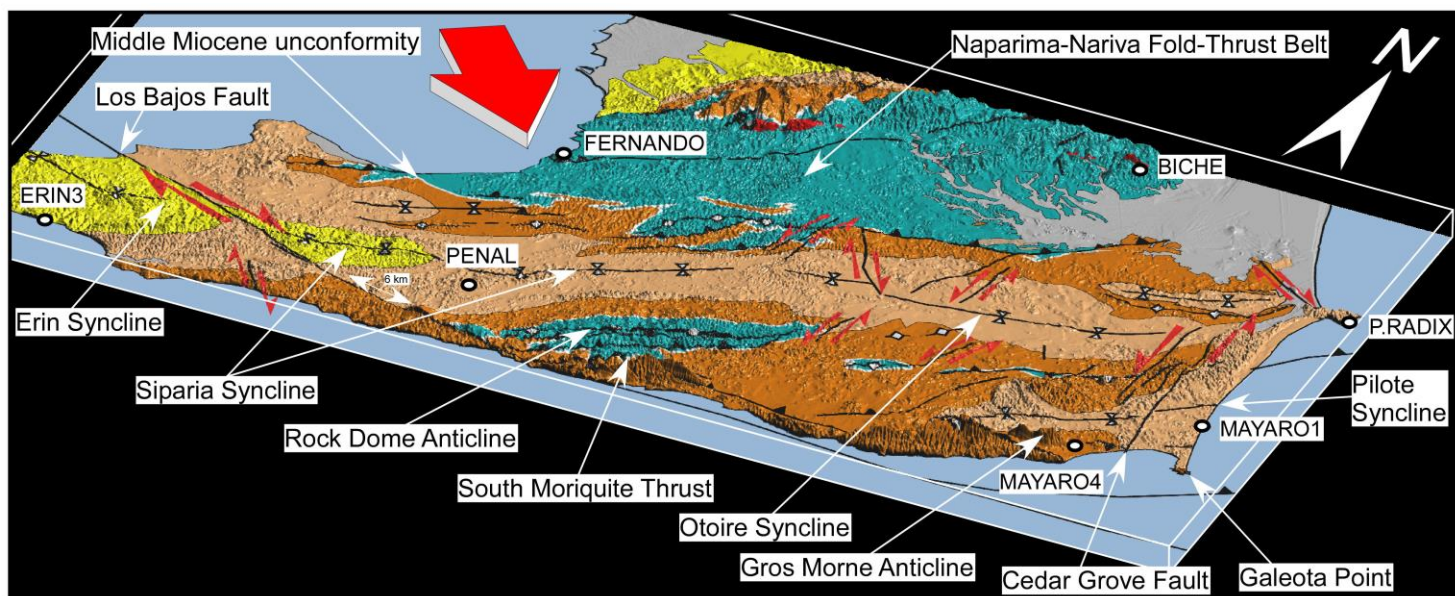


Figure 4. Three-dimensional view of the geologic map of the Southern Basin-Range of Trinidad taken from the larger geologic map of Trinidad overlain on topography as shown in Figure 2. All named major faults and folds are identified along with the sites where we collected paleostress information from outcrops of mesoscale faults, which showed evidence for north-northwest-south-southeast compression. The large, red arrow shows the direction of displacement that can explain the late Miocene-Pliocene structures (thrusts, folds, and strike-slip faults) and the stress field of Figure 9.

III- FAULT KINEMATIC METHODS

To better characterize and understand the evolution of this part of the southern Caribbean margin during the Neogene, we collected fault kinematic data in Neogene stratigraphic units and characterized the tectonic structures by inverting fault-slip data for paleostress orientations. Methods of brittle fault kinematics analysis and paleostress reconstructions are widely used in tectonic analysis (e.g., Célérier et al., 2012). We used software developed by Angelier (1990). Our fault kinematic results are reported in Table 1.

For determining paleostresses, we measured striated fault planes with clear senses of movement in Neogene rocks (Table 1). This was a challenging task because Trinidad's tropical climate and dense vegetation result in only sparse rock exposures. Furthermore, tropical weathering rapidly obscures the striation and the shear-sense indicators that are generally best preserved on fresh outcrops. In the end, our analysis was successful largely because of finding relatively fresh rock in quarries and along wavecut exposures along coastlines (Figure 2). We used fault-slip data to compute paleostresses and characterize the observed brittle mesostructures in terms of stress orientations. By working with rocks of a variety of ages, this method allows one to reconstruct the paleostress evolution. Then, one can check compatibility of structures with dated paleostress fields.

Paleostress analysis is based on the assumption that slickenside lineations and shear indicators on a fault plane indicate both the direction and sense of maximum resolved shear stress on that fault plane. By measuring the slip directions and hence the shear stress orientations of fault planes of various orientations, one can determine an average "reduced" stress tensor (Carey and

Brunier, 1974; Angelier et al., 1982). A reduced stress tensor is characterized by four variables: the orientations of the three principal stress axes σ_1 , σ_2 and σ_3 , and a ratio $\Phi = (\sigma_2 - \sigma_3) / (\sigma_1 - \sigma_3)$ (Table 1). To determine these four variables, one needs at least four fault slip measurements. To increase accuracy, using at least 10–20 fault slip measurements is best. Moreover, to best constrain the trend of the stress axes, measuring faults with opposite slips (i.e., conjugate or antithetic faults) or faults with various orientation works well (Hippolyte et al., 2012).

Because the direction and sense of slip on a fault plane depend only on the stress tensor and the orientation of the fault plane, one can use fault planes of various scales to characterize the stress tensor. Generally, the mesofaults that can be observed in outcrops ranges in scale from 10 cm (4 in.) to a few tens of meters (tens of feet). Because the stress field controls the fault slips at all scales, paleostress analysis then allows interpretation of mapped structures.

In this study, we characterize the tectonic paleostresses responsible for the Neogene geodynamic evolution of Trinidad. Striated faults are usually measured in brittle rocks like limestone in which senses of slip can easily be determined from calcite steps or stylotites. Therefore, we primarily studied outcrops of the middle Miocene Guaracara Limestone Member of the Tamana Formation.

The upper Neogene sequence of Trinidad mainly consists of clay and sand, in which sense of slip is rarely preserved by calcite fibers. For these soft rocks we mainly used observations of stratigraphic separations to determine the senses of fault slip. As shown in Figure 5, stratigraphic separation can be used to determine the sense of slip of normal faults, of reverse faults, and in some cases of strike-slip faults.

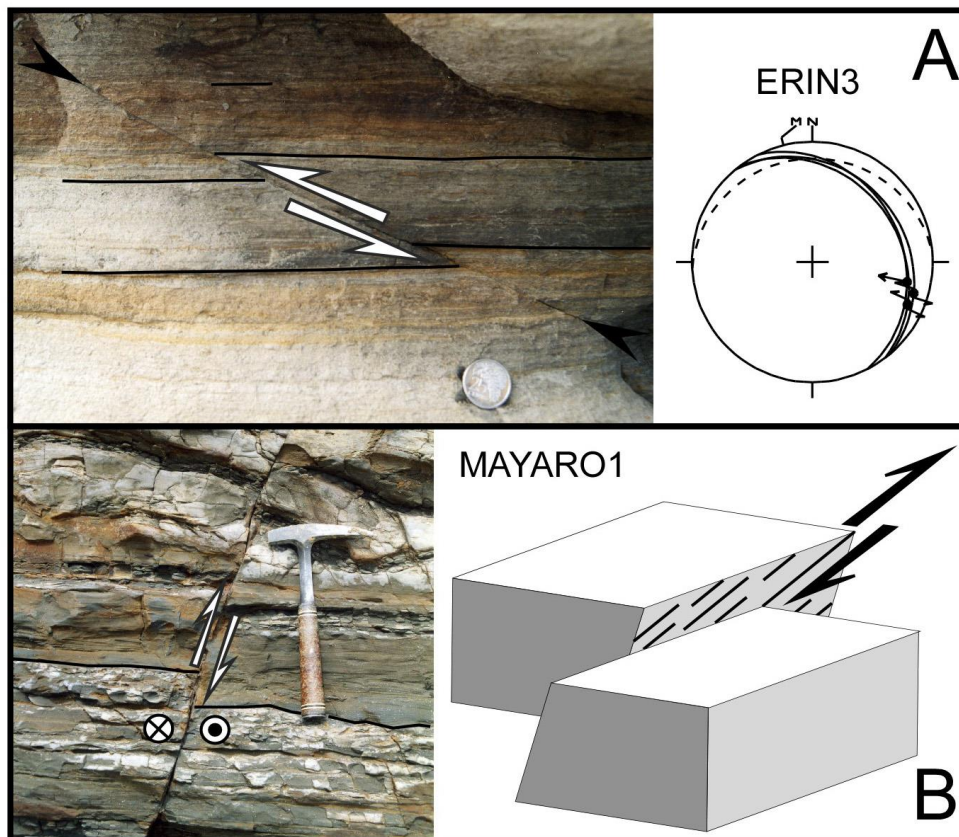


Figure 5. Field examples of mesoscale faults showing the structural criteria used for determining fault senses in Pliocene clay and sand. (A) At site Erin3, minor fault with 3 cm of reverse offset of clay layers. Lower hemisphere Schmidt's diagrams show orientations of reverse faults and bedding plane, shown as a dashed line. (B) At site Mayaro1, the right-lateral sense of an east-striking fault is inferred from its reverse component (cf. fault diagram in Figure 7). Both the Erin3 and Mayaro1 sites indicate west-northwest–east-southeast shortening as indicated by the large arrows in Figures 7 and 12.

To compute paleostresses, we used the “direct inversion” method of Angelier (1990, 1994). Most methods used for paleostress determination are based on minimization of the angle between the computed slip vector and the observed striation. The direct inversion method also minimizes the relative friction on the faults and, therefore, is accurate, even in the case of conjugate faults. The quality of the result is controlled by two values: ANG and RUP (Angelier, 1990, 1994; Table 1). ANG (from 0° to 180°) describes the misfit angle between the actual slip and the theoretical shear stress; RUP (from 0% to 200%) depends on both the misfit angle and the relative shear stress magnitude. Results are acceptable for individual values of ANG between 0° and 22°, RUP values below 75%, and average ANG and RUP values below 20° and 50%, respectively (Angelier, 1990). Our results are listed in Table 1. Faults and stress axes are also shown in lower hemisphere Schmidt diagrams of Figures 5, 6, 7, 9, 10, 12, 13, 14, and 15.

IV- RESULTS OF BRITTLE FAULT ANALYSIS

We mainly studied faults in the Neogene sedimentary sequence corresponding to the timing of the main deformation phases or stages in Trinidad. Striated fault surfaces were measured at 20 sites in the Central Range and in southern Trinidad (Figure 2). In the Central Range, we mainly worked in the Guaracara Limestone Member of the Tamana Formation, which is of middle Miocene age. Rocks above and below this limestone were generally not exposed. One additional isolated quarry containing an outcrop of an older, upper Cretaceous limestone (Naparima Formation) was studied at San Fernando (Figure 2; site Fernando).

IV-1- Polyphase Neogene Deformation

Some of the sites studied showed polyphase deformation. We computed 31 paleostress tensors (Table 1). We found extensional, strike-slip, and compressional stress regimes. Site P. Manza, located in the Central Range and along the southern shore of Manzanilla Point, provides a good example of a site recording polyphase deformation (Figures 2, 6). We measured striated fault planes in a sandy limestone layer situated below the black siltstones of the Manzanilla Formation that we assigned to the Guaracara Limestone Member of middle Miocene age (Figure 6). The limestone dips 42° to the north-northwest and is the eastern prolongation of the Guaracara limestone outcropping at Brigand Hill (Figure 6).

The striated fault surfaces measured at this site cannot be modeled with a single stress tensor, which indicates that deformation is polyphase. We distinguish conjugate reverse faults, conjugate normal faults, and strike-slip faults (Figure 6). All these faults are consistent with east-northeast-trending compression, east-northeast-trending extension, and strike-slip state of stress with south-southeast-trending compression. The sigma 3 axis (σ_3) has the same trend for the extensional and strike-slip states of stress. These two states of stress are related through a permutation of the sigma 2 (σ_2) and sigma 1 (σ_1) axes. This permutation may occur during a single tectonic event, as shown by previous studies (Hippolyte et al., 1992). In Trinidad, most of the sites with strike-slip deformation also showed normal faulting with extension perpendicular to the

compressional axis. The systematic associations of strike-slip and normal faults, with stress permutation relationships, strengthen our interpretation in which this extensional deformation in Trinidad is mainly related to strike-slip deformation.

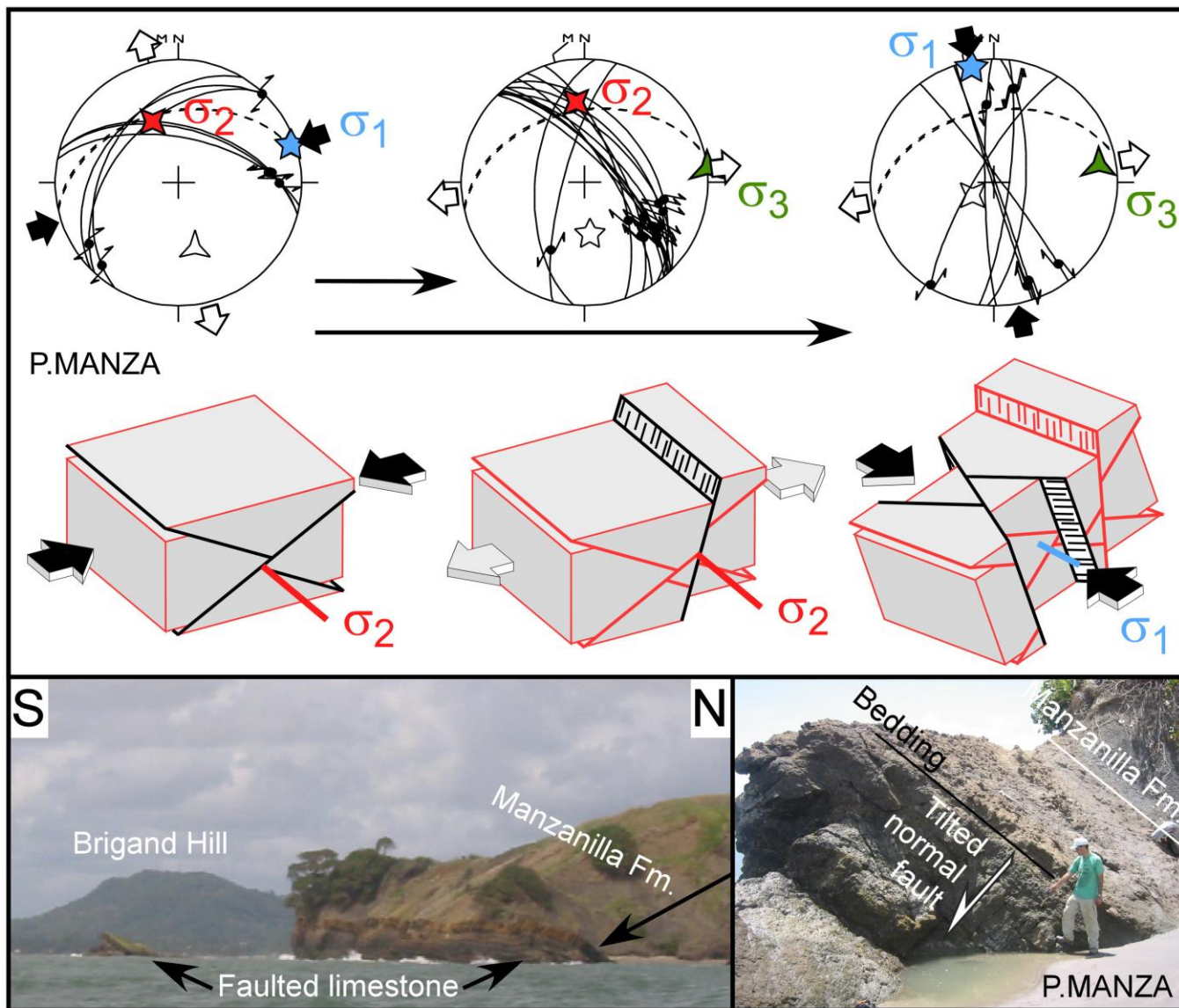


Figure 6. Example of determining fault chronology from tilting. At site P. Manza, conjugate reverse faults and normal faults have been tilted to the north by folding along the northern slope of the Central Range. To the right, strike-slip faults produced during north–south compression show tilted and horizontal striae that occurred during folding and postdates the east–northeast–trending compression. The extensional deformation is related to north–south compression through a permutation of the sigma 2 (σ_2) and sigma 1 (σ_1) axes. The sigma 3 axis (σ_3) of the east–northeast–trending extension has the same orientation as the sigma 3 axis (σ_3) of the north–south compression (cf. Hippolyte et al., 1992). The lower hemisphere Schmidt's diagrams show the measured faults and the computed stress axes (five-branch star = σ_1 or maximum principal stress axis; four-branch star = σ_2 or intermediate principal stress axis; three-branch star = σ_3 or minimum principal stress axis. Bedding planes are shown as dashed lines.

IV-2- Chronology of Compressional Faulting

Among the 31 stress tensors that we computed from fault-slip data measured in the field in Trinidad, 22 are compressional to strike-slip. The trends of compression belong to three groups: east-northeast–west-southwest (azimuth 73° in average), north-northwest–south-southeast (azimuth 169° in average) and west-northwest–east-southeast (azimuth 122° in average; Figure 7). This suggests that the stress field changed through time. This hypothesis is supported by the finding of polyphase compression at five sites: Mayaro, P. Manza, Bacha2, Mayo1, and Biche (Figure 7). Among them, site Mayo1 recorded all three trends of compression. The record of the three trends of compression in a single site confirms that Trinidad underwent at least three successive tectonic events.

In fault-slip studies, the chronology of faulting is commonly determined by observation of superposed slickensides on a fault plane. When the bedding planes have been tilted, one can also determine the occurrence of faulting relatively to this tilt. According to Anderson's (1951) theory of faulting, the principal stress axes are generally either horizontal or vertical. Two of the three perpendicular principal stress axes them have to be nearly horizontal, parallel to the surface of the Earth, and the vertical principal stress axis is parallel to the earth's gravitational field. Therefore, one of the reconstructed paleostress axes generally records the paleo-vertical. In folded rocks, one can identify tilted paleostress axes from nontilted paleostress axes and determine their chronology. Frequently, this relative chronology can be hypothesized in the field by the attitude of the striation. For neo-deformed Andersonian faults, the observed striation is generally either parallel or perpendicular to the intersection of the fault with the horizontal surface, that is, either dip-slip or strike-slip (Figure 6). Consequently, in folded rocks, it is sometimes possible to distinguish striations that formed before tilting (parallel or perpendicular to the intersection of the fault with the bedding plane), from striations that formed after tilting (frequently horizontal or down the dip and in the plane of the fault) or during the tilt (both types and intermediate striation). These geometrical relationships have proven very useful in folded areas to determine the chronology of faulting events (e.g., Hippolyte and Sandulescu, 1996; Hippolyte et al., 2012; and Homberg et al., 2013).

Site P. Manza, along the northern flank of the Central Range, where bedding dips to the north, illustrates such a chronological relationships (Figures 2, 6). The first diagram of Figure 6 shows tilted conjugate reverse faults, the second shows tilted conjugate normal faults, and the third shows faults with tilted (parallel to bedding) and nontilted (horizontal) strike-slip striation. We infer that the north-northwest–south-southeast compression occurred during folding and that the east-northeast-trending compression predates the tilt and this compression. We conclude from site P. Manza that reverse faulting characterized by east-northeast–west-southwest compression was followed by a second tectonic phase. This second phase was characterized by strike-slip deformation with north-northwest–south-southeast compression, transient stress permutation (normal faulting) and tilting to the north of the Miocene units (Guaracara and Manzanilla Formations; Figure 6) related to the structural uplift of the Central Range (Figure 2).

Similarly, the relationship between faulting and tilting at site Mayo1, indicates that the north-northwest–south-southeast compression was followed by the west-northwest–east-southeast compression (Figure 7). Using additional relationships like these, we infer the following chronology of compressional events: (1) east–northeast-trending compression, (2) south–southeast-trending compression, and (3) east–southeast-trending compression.

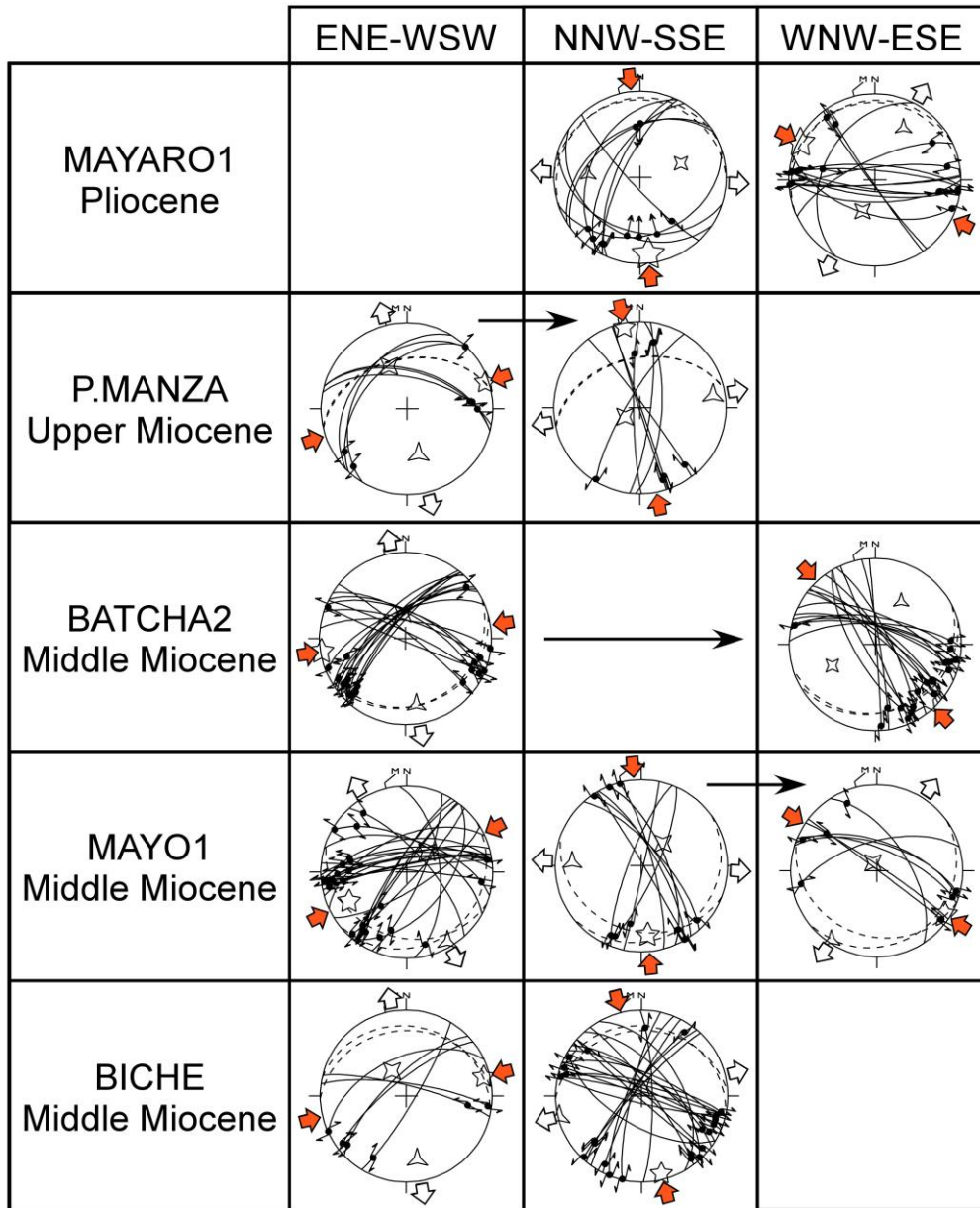


Figure 7. Compilation of fault sites in Trinidad that show polyphase deformation. Arrows indicate the chronology based on observation of tilted faults as illustrated by the method shown in Figure 6. Three successive compressional events with different trends are recorded within the Neogene sedimentary formations.

IV-3- Stratigraphic Dating of Tectonic Events

To stratigraphically date these compressional events, we measured faults in various stratigraphic units of the Cenozoic sequence. For example, we checked to see whether the faulting events identified in the middle Miocene limestones also affected younger rocks. The age of a tectonic event cannot be any younger than that of the most recent affected stratigraphic units. In Figure 8, we report the names of the faults-slip study sites in front of the affected stratigraphic unit for the three compressional events. It is clear from this figure that the east-northeast-west-

southwest compression, which is the oldest event, did not affect rocks above the middle Miocene unconformity. Sites Batcha2, Mayo1, and Biche are in the middle Miocene Guaracara limestone. Site P. Manza is in a carbonate layer situated below the Manzanilla Formation (Figure 6) that is not biostratigraphically dated but should be of similar age based on the observation that it records the same fracturing history as the three other sites. We infer that east-northeast compression is that of the main tectonic event that strongly deformed rocks in Trinidad before formation of a major unconformity and deposition of the upper Miocene sediments.

The second compressional event, a north-northwest–south-southeast compression, affected upper Miocene and Pliocene units. Site Mayaro1 in the Mayaro Formation and site Penal in the Morne L'Enfer Formation indicate that south-southeast-trending compression occurred up to the early Pliocene (Figure 8). Site Erin3 suggests that it also affects the Erin Formation of late Pliocene age. The direction of compression is poorly constrained in this site because of the lack of conjugate faults, but our four right-lateral slip measurements (Figure 9), and the observed right-lateral stratigraphic offsets on the Los Bajos fault with the same orientation, suggest that this event occurred up to the late Pliocene in southern Trinidad.

The third compressional event clearly affected all stratigraphic units up to the Erin Formation and is observed at sites Fortin2, Erin1, and Erin3 where we do not have enough faults to compute a state of stress (Figure 8, Table 1). We infer a Quaternary age for this tectonic event. The west-northwest trend of this compression is in agreement with the present right-lateral slip of the Central Range fault that is oriented east-northeast–west-southwest.

The exact timing of the transition from the second to the third compressional event is only constrained at site Erin3 (Figure 8). Moreover, this timing is mainly valid for the Southern Basin where we studied the Mayaro and Erin Formations and it may have occurred earlier in central and northern Trinidad.

Babb and Mann (1999) used stratigraphic data to show that the Gulf of Paria basin opened during the middle and late Pliocene. This likely occurred by the gradual transfer of slip from the El Pilar fault zone to the Warm Springs and Central Range fault system that we infer moved during the third compression. The El Pilar fault zone, whose right-lateral slip is compatible with the second compression, was active during the late Miocene, contemporaneously with the deposition of the Cunapo conglomerate that results from the erosion of the top of the Northern Range or Northern Range equivalent hinterland rocks, up to the end of deposition of the Springville Formation, in the middle Pliocene (Babb and Mann, 1999; Figure 3). We conclude that, in Trinidad, the transition from north-northwest–south-southeast to west-northwest–east-southeast compression gradually occurred during the middle Pliocene to early Pleistocene period. In summary, after a middle Miocene contractional event, deformation occurred under north-northwest–south-southeast compression during the late Miocene and middle Pliocene and west-northwest–east-southeast compression during the Pliocene–Quaternary (Figure 8).





EPOCH		ENE-WSW (N73E) 	NNW-SSE (N169E) 	WNW-ESE (N122E) 
Pleis.				
Plioc.	ERIN		Erin3	Fortin2 Erin1
	M. L'ENFER FOREST	MAYARO	Penal Mayaro1	Mayaro1
Late Miocene	CRUSE LENGUA	MORUGA	P.Radix Mayaro4	
MIDDLE MIOCENE UNCONFORMITY				
Middle Miocene		P.Manza Batcha2 Mayo1 Biche	P.Manza Mayo1 Biche	Brigand Batcha1 Batcha2 Mayo1 Mayo2 Gaspari
Early Miocene				

Figure 8. Stratigraphic constraints on the ages of the three compressional events summarized in Figure 7. The names along the right side of the table are the fault sites where the events were documented. The east-northeast–west-southwest compression is not recorded in rocks younger than the middle Miocene unconformity. Site Erin3 suggests that north-northwest–south-southeast compression continued up to the late Pliocene in southern Trinidad. The west-northwest–east-southeast compression occurred during the Quaternary and is compatible with active, right-lateral, strike-slip along the Central Range fault that is known from both fault trenching and GPS studies. GPS = global positioning system.

V- NEOGENE TECTONIC EVOLUTION OF TRINIDAD

The reconstructed stress field evolution of Trinidad allows the recognition of three steps in the Neogene development of this fold–thrust belt.

V-1- Phase 1, Middle Miocene East-Northeast Compression

Large magnitude deformation occurred in Trinidad before deposition of late Miocene sedimentary units (Soto et al., 2011). Structures generated during this event are not clear on geological maps, but the widespread middle Miocene unconformity, recognized offshore and onshore, can be related to Phase 1 compression, which also occurred during the middle Miocene. In the field, we could recognize this early event via pretilt reverse faults (site P. Manza) and strike-slip faults (sites Batcha2, Mayo1, and Biche; Figure 7). Trends of compression are uniformly east-northeast–west-southwest. This trend is inconsistent with the present right-lateral geodynamics of the southern Caribbean plate boundary zone. Right-lateral displacement along an east–west fault should result from compressional stresses oriented around northwest–southeast. As the magnitude of Miocene deformation was large during the middle Miocene, we suspect that these

early-formed faults have been rotated by block rotations about vertical axes. Assuming that the stress axes have always been consistent with right-lateral displacements along the South Caribbean margin, approximately 90° clockwise block rotations or approximately 45° counterclockwise block rotations are needed to restore the observed east-northeast–west-southwest paleostress axes to northwest–southeast or north-northwest–south-southeast orientations.

There are sparse paleomagnetic data to support that such block rotations occurred in Trinidad. Giorgis et al. (2008) attempted to calculate the amount of finite strain that has accumulated across the active Central Range fault zone since the Miocene and their data suggest counterclockwise and $35^\circ \pm 11^\circ$ clockwise rotations. Paleomagnetic data from rocks of Cretaceous age suggest large clockwise block rotations about vertical axes occurred sometime post-late Cretaceous along the entire length of the Caribbean–South American plate boundary (Skerlec and Hargraves, 1980; Stearns et al., 1982; and Burmester et al., 1996). On Tobago, at the eastern end of a Mesozoic igneous belt along the Caribbean–South American plate boundary zone, volcanoclastic sediments and dykes of Albian age indicate that these rocks have been rotated approximately 90° clockwise (Burmester et al., 1996). This rotation occurred before the Pliocene because the middle Pliocene Rockley Bay Formation was not rotated (Weber et al., 2014). In the Caribbean Mountains of northern Venezuela, easterly declinations in Cretaceous intrusive rocks suggest average 90° clockwise rotations of crustal blocks about vertical axes; this was attributed to late Cretaceous deformation (Skerlec and Hargraves, 1980).

In Trinidad, the east–northeast-trending compression discussed above was recorded in the Guaracara Limestone Member of Miocene age (Figure 3). The presumed rotation should postdate the deposition of this limestone, which contains the faults studied. As it requires large magnitude deformation, most of this rotation likely predates the middle Miocene unconformity. The suspected age for the hypothesized rotation is thus middle Miocene. This age is consistent with the timing of the arrival of the Caribbean arc along the South American plate at the longitude of Trinidad.

Without additional structural data, it is not possible to conclude whether the possible block rotations resulted from a megatectonic rotation as suspected for the rotations in the Cretaceous rocks (Skerlec and Hargraves, 1980), or from in situ rotation of numerous small blocks (e.g., Nelson and Jones, 1987). As the South Caribbean margin is today, and has been much of the Neogene, a generally right-lateral strike-slip boundary, clockwise block rotation should be expected, even during the Neogene. Large block rotations, of more than 90°, can occur when the brittle upper crust is broken into small blocks, and these rigid blocks rotate independently in response to continuous ductile deformation at greater depth (Nelson and Jones, 1987). Right-lateral slip along bounding faults can result in a dextral sense rotation of fault blocks (e.g., MacDonald, 1980). The more intense deformation recorded in the upper Oligocene–middle Miocene rocks of Trinidad (Soto et al., 2011) and the discontinuous outcrops of the Guaracara Limestone Member that suggests tectonic separation of faulted blocks (Mayo, Bacha, Biche, and Brigand in Figure 2) argue for this model.

However, large clockwise rotation of a coherent mass cannot be excluded. Some models predict that large rotation can better be explained by rotating a structural coherent mass than simple shear associated with strike-slip faulting (e.g., Skerlec and Hargraves, 1980). A combination of both processes is also possible. Even if a diachronous rotation mechanism driven by the relative motion of the Caribbean plate is recognized (e.g., Beardsley and Avé Lallemant, 2007), these questions remain open and in need of resolution by further paleomagnetism and structural analyses in Trinidad.

V-2- Phase 2: SSE Compression, Folding, Thrusting, and Strain Partitioning

The south-southeast-trending compression, of late Miocene–middle Pliocene age, is compatible with most of the structures of the Southern Range, Southern Basin and Central Range of Trinidad (Figures 2, 9). This compression trend is normal to the axes of most of the synclines and anticlines and thrusts mapped there. For example, we found this trend of compression at site Mayaro4 where bedding planes dip 40° to the south, and where tilting occurred during faulting and north-vergent thrusting (cf. the pretilt and posttilt striation in the diagram Mayaro4 of Figure 9). Note that, even if the fault slips were measured in a north-vergent fault-bend fold (Figure 4), the fault diagram mainly shows strike-slip faults. Generally, in fault slip studies, shortening is more often represented by strike-slip state of stress rather than a compressional state of stress. The main reasons for this bias is that shortening is usually mainly accommodated by folding and strike-slip faulting and that reverse faults are less frequently exposed in outcrops.

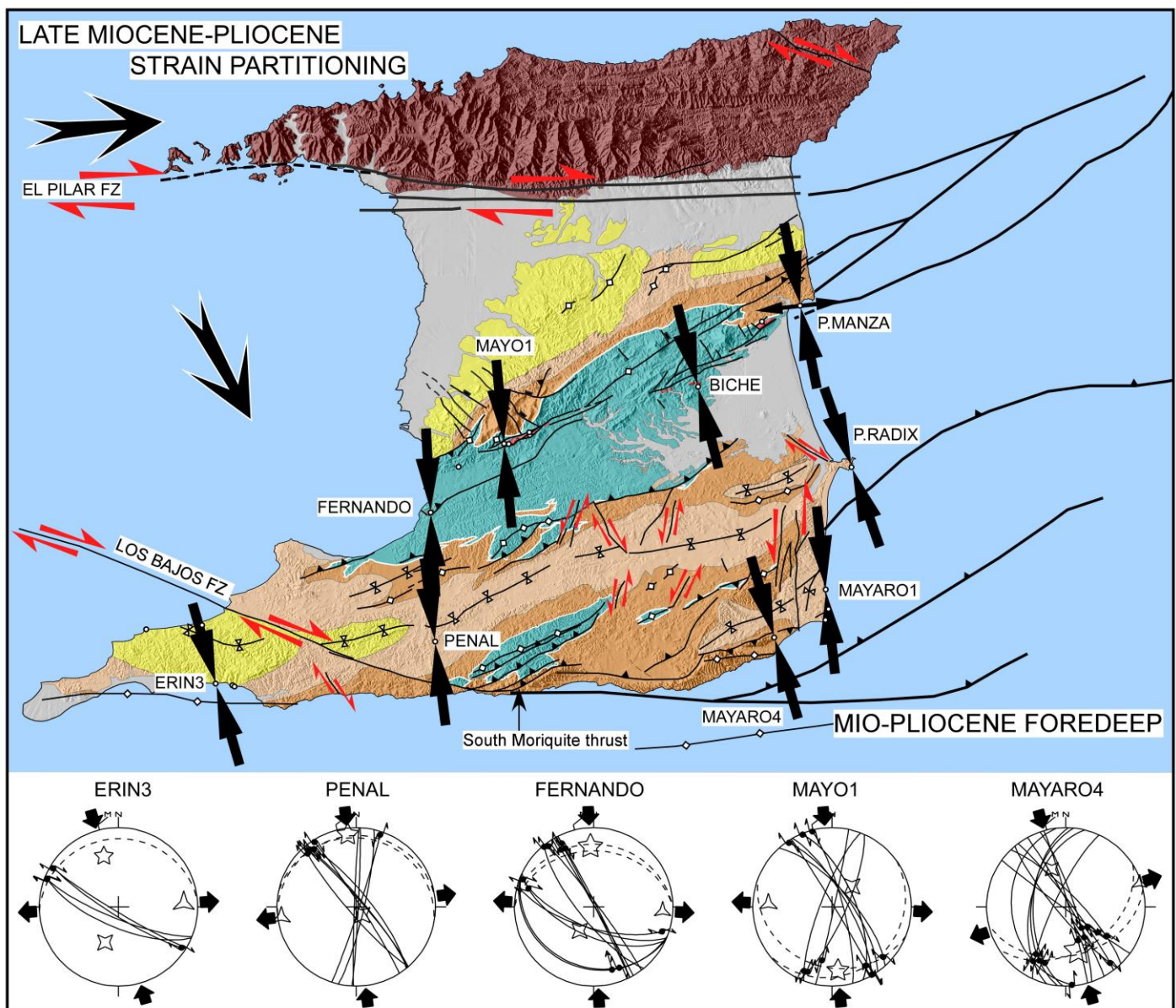


Figure 9. Late Miocene to middle Pliocene structures and stress field in Trinidad. south–southeast-trending compression is responsible for most of the tectonic structures mapped on Trinidad (Figure 2). We attribute to this phase the subsidence in the Northern and Southern basins and most of the south-verging thrusts. In southern Trinidad we interpret oblique faults, including the Los Bajos fault, as right-lateral and left-lateral oblique ramps (red harpoon arrows). The transpressional uplift of the Northern Range and the activity of the El Pilar fault zone are attested at this time by the deposition of the Cunapo conglomerate. The right-lateral sense of slip of the El Pilar fault zone is compatible with the north-northwest–south-southeast trend of compression. There was strain partitioning between this strike-slip motion and the thrusting occurring in Central and Southern Trinidad. The two large black arrows show a displacement partitioning that can explain the structures and the stress field over the island of Trinidad.

The north-northwest–south-southeast trend of compression is also compatible with right-lateral and left-lateral slips on oblique ramps associated with thrusts in southern Trinidad (Figures 4, 9). For example, at Point Radix, strike-slip faulting of this compressional stage occurred during a 40° southern tilting of the Mayaro Formation, which is of Pliocene age (Figure 10). At this site, like at sites Mayaro2 and Mayaro3 (Table 1), we found normal faults related to north-northwest–south-southeast extension that predates folding (Figure 10). We interpret this north-northwest–south-southeast extension, which occurred only locally in the Southern Basin, to be a response to flexural deformation in a foredeep basin in front of the Central Range. At site P. Radix, two families of conjugate normal faults have been tilted to become low-dipping normal faults and subvertical normal and reverse faults (Figure 10). The south–southeast-trending compression reactivated east–northeast-trending extensional faults in a left-lateral sense and created new strike-slip faults. That strike-slip striation is either parallel to the bedding plane or horizontal (cf. the lower fault diagrams of Figure 10), shows that the southward dip of the bedding planes results from this compression. At site P. Radix, we ascribe this compressional deformation to south-vergent thrusting at the southern tip of a right-lateral oblique ramp (Figure 9).

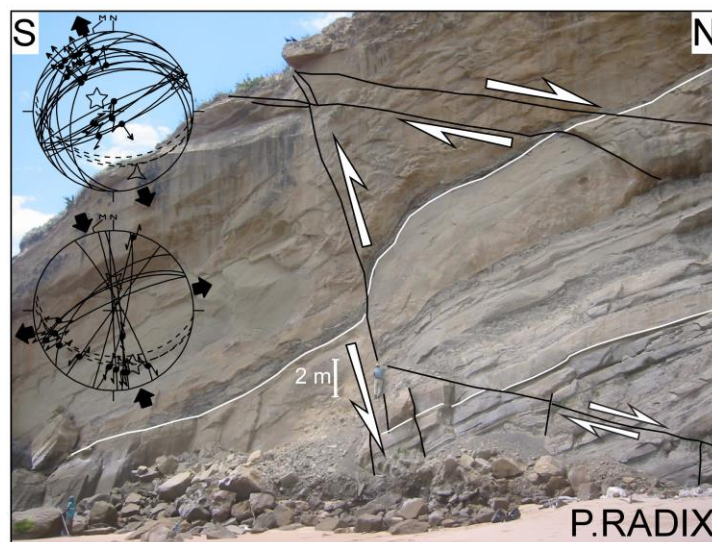


Figure 10. Example of pretilt conjugate normal faults in the Moruga (upper Miocene) Formation. The measured striated normal faults and the computed extension are shown in the upper diagram. Three sites (P. Radix, Mayaro2, and Mayaro3 summarized in Table 1) showed early, north–south extension. This early deformation may represent foreland flexuring or compaction during shortening in the Central Range. It was followed by folding during north-northwest–south-southeast compression that reactivated the normal faults with left-lateral slip as shown in the lower diagram.

In southeastern Trinidad, older maps (Kugler, 1959; Persad, 1984; Saunders, 1998) show that the Mayaro area was affected by north–south faults, for example, the Cedar Grove fault, which has been interpreted as either a left-lateral strike-slip fault (Persad, 1984) or a normal fault (Bowman and Johnson, 2014). We found no evidence for normal faults in this orientation while making observations along the coastline. Our structural and stress field analysis suggest that the mapped onshore north-trending faults could be left-lateral strike-slip faults related to the fold–thrust system developed in the Southern Range during south-southeast-trending compression (Figures 4, 9).

In southwestern Trinidad, Los Bajos fault may offset right-laterally by approximately 6–10.5 km (~4–6 mi) the Erin syncline from the Siparia syncline (Figure 9). In neighboring sites, Erin3 and Penal, we found right-lateral strike-slip faults that trend parallel to the Los Bajos fault and, which also correspond to the north-northwest–south-southeast compression (Figure 9). That similar trends of compression characterize north–west-trending strike-slip faults (sites Erin3 and Penal), and the folds and thrusts of southeastern Trinidad (sites Mayaro4 and Mayaro1), supports the interpretation that Los Bajos strike-slip fault is an oblique ramp of the thrust system of the Southern Range (South Moriquite and Moreau Road thrusts, Rock Dome anticline; De Verteuil et al., 2006; Figures 4, 9).

The east-northeast-trending synclines of southern Trinidad involve the Pliocene sandstones of the Mayaro and Erin Formations, which confirms the proposed late Miocene–Pliocene age of the south-southeast-trending compression (Figure 4). In the Central Range, we found this trend of compression at sites P. Manza, Mayo1, and Fernando. At site P. Manza, at the Manzanilla Point, this compression is clearly related to the northward tilt and structural uplift of the northern flank of the Central Range (Figures 6, 11).

Site P. Manza is the only site of south-southeast-compression where we found stress permutation and extension, whereas stress permutation and extension are common for the younger stress field. Paleomagnetism measurements from upper Miocene sandstones and shales of the Manzanilla and Springvale formations suggest approximately 35° of clockwise rotation near this site (Giorgis et al., 2008). It is thus possible that faults measured at site P. Manza have been rotated clockwise and that the south-southeast-compression at this site was originally trending northwest–southeast. Local clockwise rotation is possible because this site is situated at the left step between the Central Range and the Caigual strike-slip faults (Figure 11). The original trend of compression may have been like that at Brigand Hill (Figure 12).

At site Fernando, this compression is characterized by multiple flat shears in the thinly bedded Cretaceous limestone, and we relate this deformation to the Naparima Hill Thrust (Figure 11). Note that in contrast to the active Central Range fault that may be responsible for the uplift of the northern block of the Central Range, the Naparima Hill thrust that we relate to the north-northwest–south-southeast compression, does not have a clear morphological expression and is not active at present (Figure 11). Conversely, the Central Range fault is presently moving with a right-lateral sense but was probably not slipping right laterally during the late Miocene because the south-southeast-trending late Miocene compression is not consistent with a right-lateral sense of slip on a northeast-trending fault.

Along the southern border of the Northern Range, the El Pilar extension shows no clear evidence of Quaternary or modern activity (Payne, 1991; Babb and Mann, 1999; and Weber et al., 2011). Seismic lines across the southern flank of the Northern Range reveal a buried positive flower structure with a fan of large reverse faults dipping north (Payne, 1991). This fault might not be currently active, but seismic lines (Payne, 1991; Babb and Mann, 1999), and sedimentology

studies (Elling et al., 2019) suggest that it was active during exhumation and erosion of the Northern Range and deposition of the Cunapo conglomerate during the Miocene and Pliocene (Figure 3). Paleocurrents inferred from maximum dip of clinoforms and thinning of the Cunapo conglomerate show that the deposition of the upper Miocene–lower Pliocene sediments reflects strong control along the northern edge of the Northern Basin (Babb and Mann, 1999). Moreover, apatite fission-track ages in the Northern Range, which give ages for exhumation through approximately 100°C, range from ca. 15 Ma in eastern Trinidad to ca. 4 Ma in the west (Denison et al., 2008).

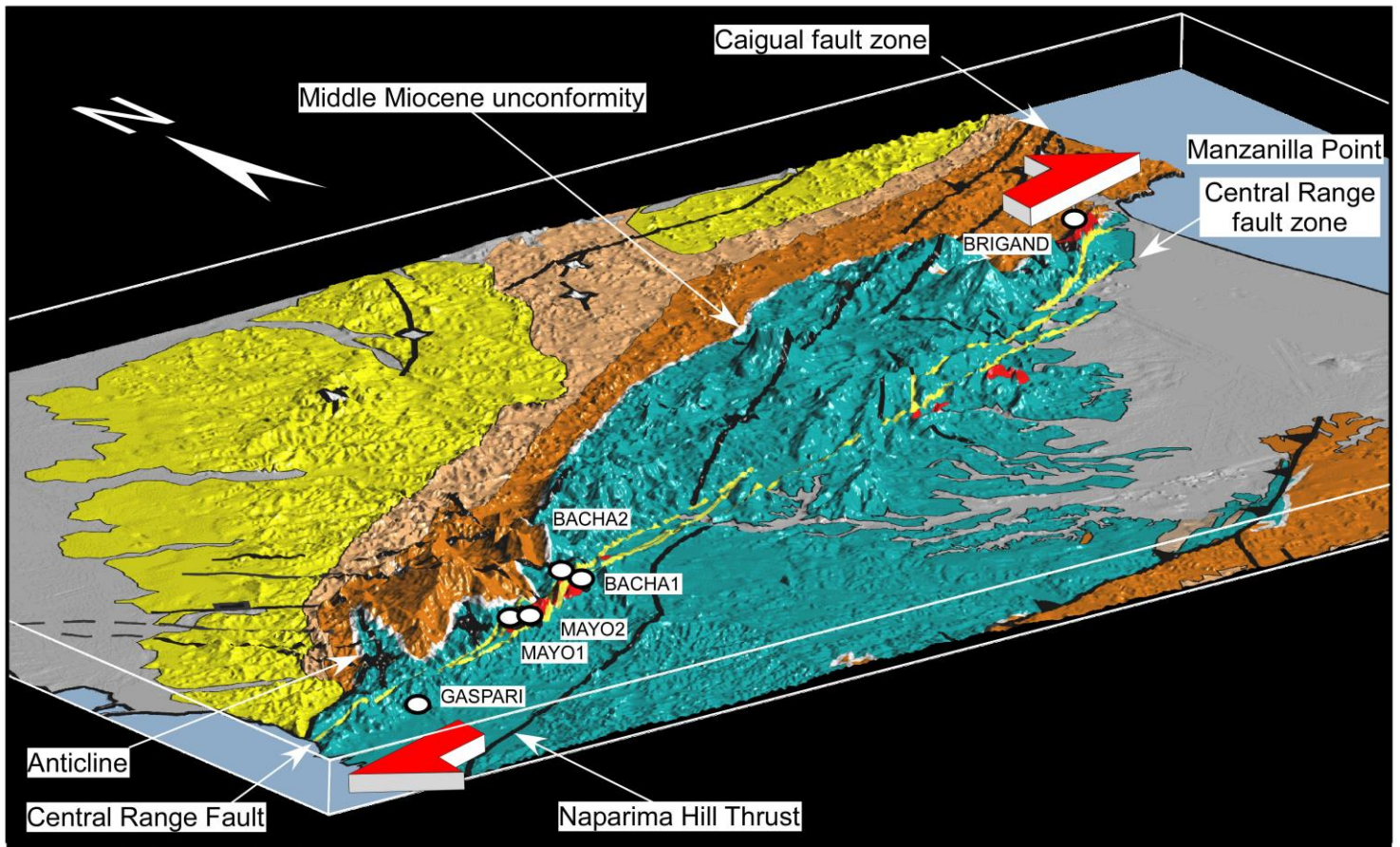


Figure 11. Three-dimensional view of the Central Range. The Central Range fault is from Weber et al. (2001a, 2011) and Prentice et al. (2010). Other fault strands of the Central Range fault zone with morphological signature are also drawn in yellow. We indicated the name of the fault sites that recorded the west-northwest–east-southeast compression compatible with the right-lateral slip (red arrows) of this active fault. Note that the present-day relief of the Central Range is limited to the south by the active Central Range fault zone and is likely the result of the modern transpressional deformation (Soto et al., 2011). South of this fault zone, there is little remnant topography inherited from older thrusting events in the pre-middle Miocene rocks. North of this right-lateral strike-slip fault zone, topography suggests active uplift. Right stepping en echelon anticlines are present near sites Gaspari and Mayo1. Perpendicular normal faults are also present next to the Gulf of Paria.

The north-northwest–south-southeast trend of compression obtained in central and southern Trinidad is compatible with right-lateral slip along the El Pilar fault zone of Trinidad (Figure 9). We infer that right-lateral slip along this fault zone and the structural uplift of the Central Range may have occurred at least within the late Miocene to middle Pliocene period. This

timing is in good agreement with the previously proposed timing of uplift for the Northern Range (Babb and Mann, 1999; Denison et al., 2008). That the north-northwest–south-southeast compression is not the present stress field would explain that the El Pilar fault zone is no longer active. It suggests that it stopped during the middle Pliocene to early Quaternary. This age agrees with the decrease in the importance of the Northern Range siliciclastic source area during the Pliocene and Quaternary (Babb and Mann, 1999; Figure 3).

Accordingly, paleostresses and structural data suggest that much of the structures of Trinidad were active during the late Miocene to middle Pliocene period (Figure 9). Whereas the Central Range, the Southern Basin, and the Southern Range were characterized by thrusts and folds, normal to the compressional stress axes, the El Pilar Fault, which on seismic lines appears like a buried positive flower structure (Payne, 1991), and which is oblique to the north-northwest–south-southeast trend of compression, was probably a right-lateral strike-slip fault like its prolongation in northern Venezuela (Persad, 1984; Saunders, 1998; Babb and Mann, 1999).

Simultaneous strike-slip and thrust displacement indicates strain partitioning separating the plate convergence vector into two components: an arc-subnormal component resulting in arc-subnormal shortening and an arc-parallel component expressed by arc-parallel strike-slip (Avé Lallemant, 1997). In Trinidad, during the late Miocene and Pliocene, strain was partitioned into an arc normal component accommodated by thrusting and folding in the Central Range and southern Trinidad and an arc parallel component accommodated by the El Pilar right-lateral strike-slip fault.

V-3- Phase 3: East-southeast Compression, Pliocene Stress Reorganization, and Strike-slip Reactivation of the Central Range

On the coast of Venezuela, Audemard et al. (2005) identified a Quaternary transpressional regime characterized by a west-northwest–south-southeast maximum horizontal stress. In Trinidad, the trend of compression rotated counterclockwise and the deformation pattern was reorganized during the late Pliocene or early Quaternary. The main change that occurred is that compression that was normal to the Central Range during Phase 2 became oblique and activated the Central Range fault zone with right-lateral strike-slip motion in Phase 3 (Figure 12).

Structural, geomorphic, and trench studies previously showed that the Central Range fault is active (Babb and Mann, 1999; Weber et al., 2001a; Prentice et al., 2010; Giorgis et al., 2011; and Weber et al., 2011). GPS sites in southern Trinidad move 14 ± 3 mm/yr slower toward the east than the predicted 20 ± 3 mm/yr plate motion and show that the Central Range fault currently accommodates 70% of the total Caribbean–South America plate motion in Trinidad (Weber et al., 2001a). GPS measurements predict that the Caribbean plate moves $20 \text{ mm/yr} \pm 3 \text{ mm/yr}$ in a direction $86^\circ \pm 2^\circ$ (Pérez et al., 2001; Weber et al., 2001a; Jouanne et al., 2011; Reinoza et al., 2015; Symithe et al., 2015). Weber et al. (2001a) inferred from the obliquity between the predicted local plate motion and the strike of the active fault that transpression is active in Trinidad and is the cause for uplift, folding and thrusting in the Central Range. The apatite fission-track study of Giorgis et al. (2017) was, however, unable to confirm that modern surface uplift and exhumation occurs in the Central Range.

The chronology of compressional events deduced from our fault study places the west-northwest–east-southeast compression as the most recent state of stress. We mainly identified this event in the Guaracara limestone, which outcrops close to the Central Range active fault (Figures 11, 12). We found it at sites Mayo1, Mayo2, Bacha1, Bacha2, and Brigand (Figure 11). Locally this strike-slip deformation tilted the Guaracara limestone (cf. diagrams of sites Mayo2, Figure 13;

Bacha2, Figure 7; Gaspari and Brigand, Figure 12). We also ascribe to this compression north–east-trending anticlines at the western tip of the Central Range fault zone and the structural uplift and tilting along the northern side of the Central Range fault zone (Figure 11).

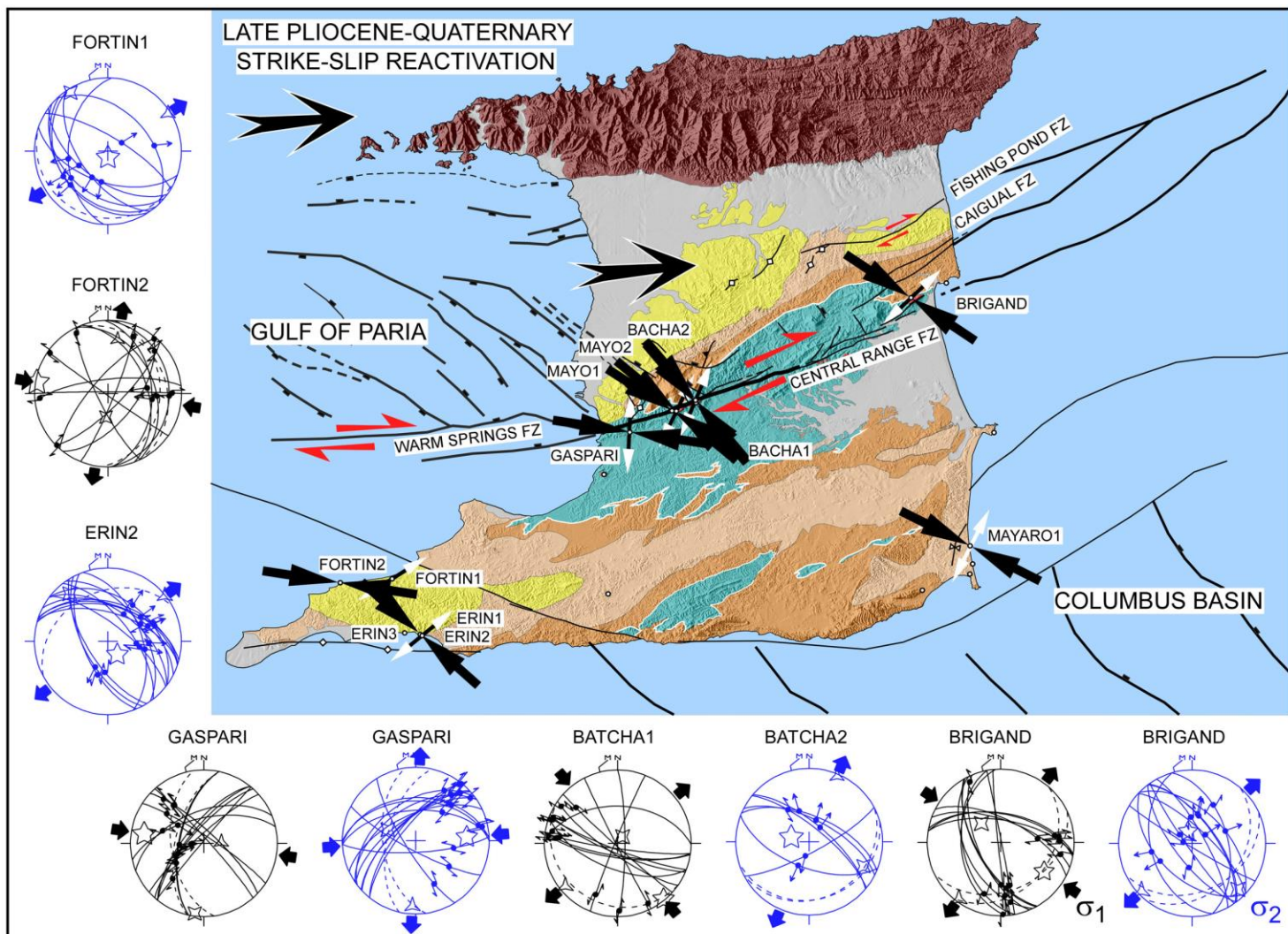


Figure 12. Late Pliocene–Quaternary deformation in Trinidad. The recent event of strike-slip deformation with east-southeast-trending compression is compatible with the right-lateral slip of the Central Range Fault. Locally compressional, strike-slip and normal states of stress are found. These three stress regimes have common east-southeast-trending maximum horizontal stress axes (σ_1 or σ_2). The restraining bend of the Central Range Fault results in uplift and folding of the northern block. Local northeast-trending extension (little white arrows and fault diagrams in blue) also occurred near the Gulf of Paria and near the Columbus Basin. The large black arrows show the present Caribbean plate motion.

Although all the sites along the Central Range fault zone show strike-slip stress regimes (Gaspari, Mayo1, Mayo2, Batcha1, Batcha2, Brigand) and folding, we also found normal faults in them (Figure 13). The sigma 3 axis (σ_3) has the same trend for the normal faulting as for the strike-slip regime (Figure 13). Strike-slip deformation and normal faulting are systematically related through stress permutation (Figure 12), which suggests that they belong to the same tectonic phase (Hippolyte et al., 1992). This can be showed at site Brigand on the northern slope of Brigand

Hill (Figure 12). The Guaracara limestone dips 36° to the southeast. We found two kinds of faults there, conjugate normal faults with minor throw (less than 50 cm), and strike-slip faults. The former correspond to northeast-trending extension, and the later correspond to strike-slip deformation with a maximum principal stress axis (σ_1) trending northwest-southeast and a minimum principal stress axis (σ_3) trending southwest-northeast (cf. diagrams in Figure 12). For the latter, strike-slip striations are either parallel to the bedding planes or horizontal. We infer that the northwest-southeast compression occurred during the tilting of the limestone. But the normal faults also show striations contemporaneous with tilting, with striations perpendicular to the intersection of the fault with the bedding plane (predating the tilting) and dip-slip striations. We conclude that normal faulting occurred through permutations of the σ_1 and σ_2 axes during folding (Figure 12). Generally, although the main deformation consists of strike-slip faulting and folding, at lower scale normal faulting related to stress axes permutation can occur, possibly at the junction of strike-slip faults (Hippolyte et al., 1992).

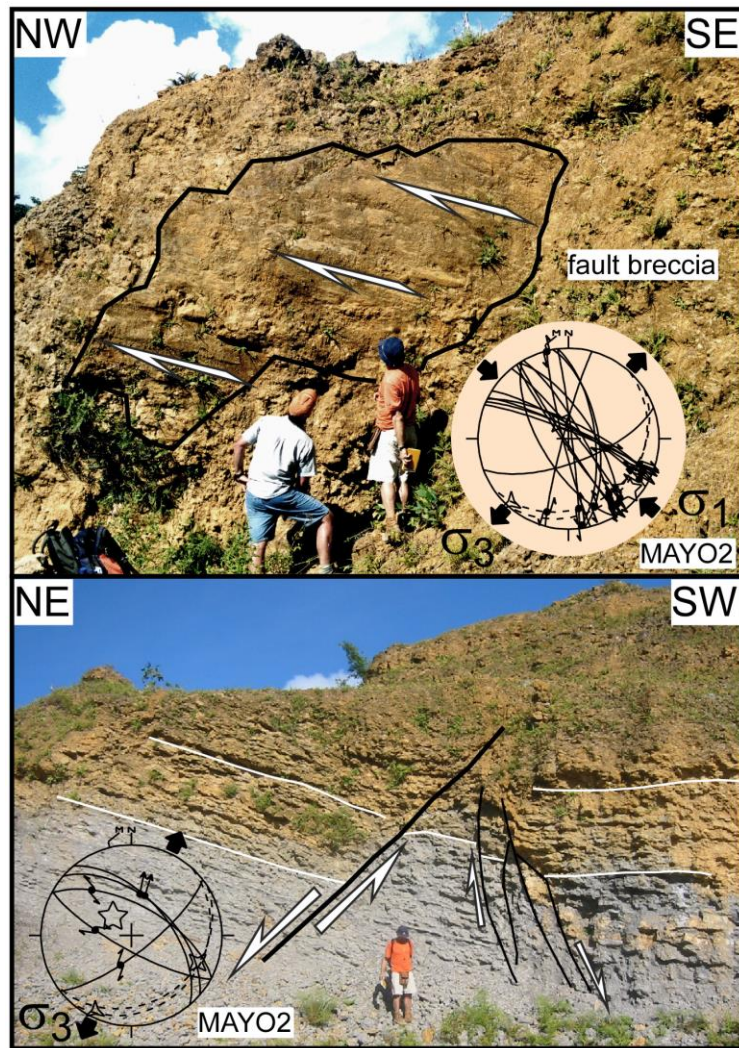


Figure 13. Strike-slip and normal faults in the Guaracara limestone of Mayo2 site, along the Central-Range fault. The main deformation is strike-slip and folding. Minor extension (lower picture) is related to the strike-slip deformation through a stress permutation and is interpreted as momentary perturbation of the stress field.

It is notable that farther from the Central Range fault zone, near the Gulf of Paria, geological maps of Trinidad show northwest-trending faults with vertical offsets (Figure 2; Kugler, 1959; Saunders, 1998; and De Verteuil et al., 2006). These faults are mapped cutting the upper Pliocene sediments of the Talparo Formation. They suggest that northeast-trending extension increases toward the Gulf of Paria where seismic lines show oblique-slip transtensional faults in the stepover area between the El Pilar fault of Venezuela to the north and the Warm Springs fault zone to the south (Babb and Mann, 1999; Figure 12).

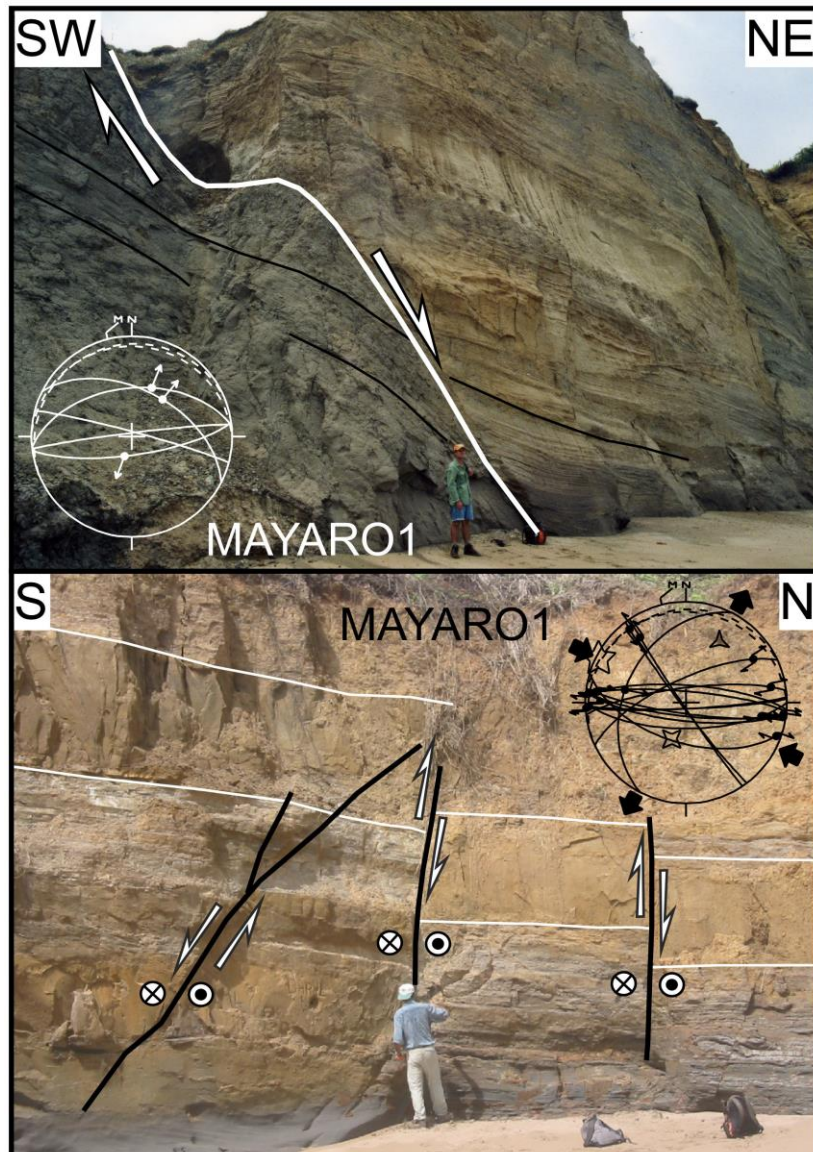


Figure 14. Strike-slip and normal faulting at site Mayaro1 in the Mayaro Formation of Pliocene age in southern Trinidad. The recent strike-slip and normal faulting initially found along the Central Range fault zone (Figure 12) also affected southern Trinidad. The lower picture shows normal faults reactivated with right-lateral slip. West-northwest-trending normal faults might be linked to the normal faults that occur in the Columbus Basin.

In southern Trinidad, we identified the west-northwest–east-southeast compression at three sites: Mayaro1, Erin1, and Fortin2 (Figure 12). At site Mayaro1, the Pliocene Mayaro Formation is cut by reverse and strike-slip faults of the south-southeast-trending compression and strike-slip faults of the east-southeast-trending compression (Figure 7). The second compression reactivates east–west normal fault with a right-lateral sense (Figures 7, 14). As discussed above, normal faulting may have various causes such as foreland flexuring, gravity, sediments compaction, or stress permutation during strike-slip deformation. Site Mayaro1 is located close to the Columbus Basin and is characterized by east- and northwest-trending normal faults (Figure 14). With only three fault measurements, we cannot compute stress axes, but a north–northeast-trending extension as indicated by the white arrow in Figure 12, is possible and would suggest stress permutation of the recent strike-slip regime. They may also be related to the gravitationally driven extensional faulting occurring in Columbus Basin (Wood, 2000; Garciacaro et al., 2011).

At site Fortin-2, we found faults in porcelainites layers within the upper Pliocene Erin Formation (Figure 12). Porcelainites are clays that have been cooked by the burning of coals. Faults are preserved in them. The sense of slip could be determined by drag folds and layer offsets. Reverse and strike-slip faults indicate that the east-southeast-trending compression affects the upper Pliocene Erin Formation, which is tilted to the east at this site (Figure 12).

Site Erin1, located on the southern side of the peninsula, confirms the Holocene age of the east-southeast-trending compression (Figures 12, 15). Conjugate reverse faults cut the sands and clays of the upper Pliocene Erin Formation. Similar reverse faults were observed at site Erin3 but without conjugate faults, so we could not compute the trend of compression at this site (Figure 5). However, the west-northwest–east-southeast trend of compression is well constrained by conjugate and oblique faults at site Erin1 (Figure 15).

The Los Bajos fault zone, whose right-lateral slip was in good agreement with the late Miocene to Pliocene south-southeast-trending compression, may not have been active during Phase 3 because with compression subparallel to the fault the shear stress would be very low. But sites Fortin2, Erin1, and Mayaro1 show that although 70% of the total Caribbean–South America motion occurs today along the Central Range fault (Weber et al., 2001a), recent deformation also occurred in southern Trinidad.

We conclude that Phase 3 affects the youngest rocks of Trinidad exposed on the south coast. East-southeast-trending compression is responsible for strike-slip faulting along the Central Range fault and likely accompanies the present-day right-lateral strike-slip motion of this fault as shown by GPS studies. A contemporaneous northeast-trending extension corresponds generally to minor deformation in the studied sites, but this stress permutation of the strike-slip regime might be related to thick-skinned extension, offshore in the Gulf of Paria at the stepover area between the Venezuelan El Pilar fault and the Warm Springs–Central Range fault zone (Babb and Mann, 1999), and to thin-skinned, gravitationally driven extension in the Columbus Basin (Wood, 2000; Garciacaro et al., 2011; Figure 12).

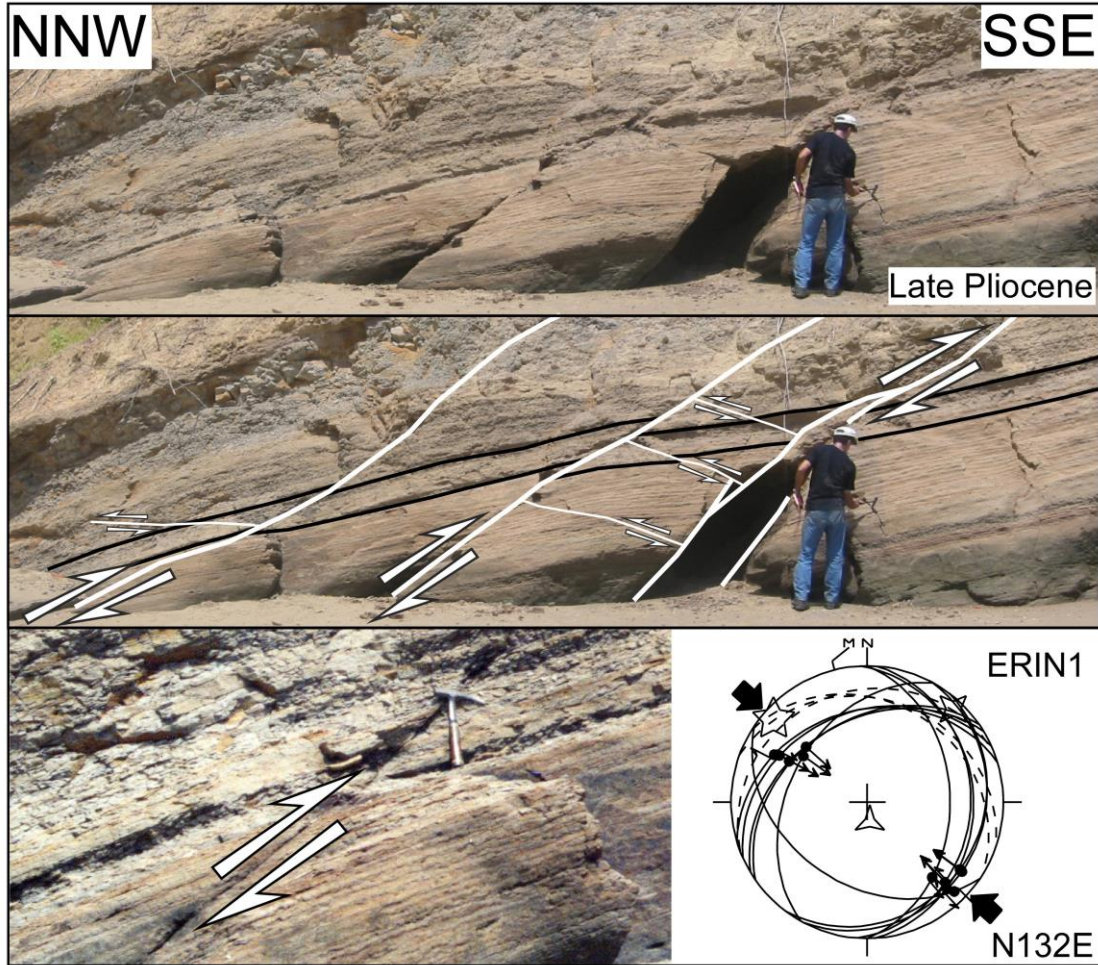


Figure 15. Conjugate reverse faults cutting the Erin Formation of late Pliocene age at the Erin1 site in southernmost Trinidad. The Quaternary compression also affected southern Trinidad (Figure 12).

VI- TECTONIC CONTROLS ON STRESS FIELD EVOLUTION IN TRINIDAD AND THE SOUTHEASTERN CARIBBEAN

Paleostresses combined with structural analysis shows that Trinidad, at the southern margin of the Caribbean plate, records a polyphase tectonic history. We identified three tectonic phases corresponding to three contrasting stress regimes. These events confirm the tectonic significance of the middle Miocene unconformity and allow to constrain the timing of strike-slip activation of the Central Range fault. The evolution of the stress field can be correlated to the rapid geodynamic evolution of the southeastern Caribbean as the Caribbean plate translated along the northern margin of the South American plate.

Babb and Mann (1999) reconstructed the Neogene structural evolution of the Gulf of Paria and Trinidad areas pointing out the progressive transfer of right-lateral motion from the El Pilar fault zone to the Central Range fault zone. More regionally, Pindell and Kennan (2001) recognized three steps in the late Cenozoic evolution in the eastern Venezuela–Trinidad area: (1) oblique

collision that occurred up to 13 Ma, (2) onset of transcurrent plate boundary development, and (3) post ca. 4 Ma right-lateral transpression across the region.

Our fault study supports the distinction of three steps of similar ages in the tectonic evolution of Trinidad, and our determined paleostress evolution is consistent with the structural evolution proposed by Babb and Mann (1999). We relate the three successive stress field stages of Trinidad to the progressive eastward displacement of the leading edge of the Caribbean plate (Figure 16).

VI-1- Middle Miocene Arrival of the Lesser Antilles Arc along Trinidad

During the Miocene, a Caribbean accretionary wedge, forearc, and arc were moving past the South American passive margin of Venezuela and Trinidad. Right-lateral oblique collision between the Caribbean and South American crusts (Pindell et al., 1998; Audemard, 2001; Audemard et al., 2005) is recorded by the eastwardly younging Caribbean foredeep basins, which started in the Paleocene at César Basin, Colombia, and continued until the middle Miocene in eastern Venezuela–Trinidad (Speed, 1985; Pindell et al., 1998).

The Trinidad region was converted from a passive margin of South America into an active margin by the oblique passage of the Caribbean arc along the passive margin during the middle Miocene (Speed, 1985; Pindell et al., 1998; Figure 16A). Sedimentation changed from deepwater passive margin Paleogene units (flysch-type sediments of the Pointe-a-Pierre and Brasso Formations Figure 3) to shallow-water active margin Neogene units. The Guaracara (Tamana) limestone indicates the first appearance of shallow-water conditions in the Central Range (Robertson and Burke, 1989; Erlich et al., 1993; Babb and Mann, 1999). Early to middle Miocene structural uplift and erosion in the Central Range is also supported by pooled apatite fission-track (AFT) ages that suggest exhumation at ca. 18–11 Ma (Giorgis et al., 2017).

Deformation occurring during the middle Miocene is likely related in Trinidad to the regional middle Miocene unconformity surface (e.g., Erlich et al., 1993). But the structures related to this event are not clearly mapped. On seismic lines, some authors showed that in the Central Range, rocks predating the middle Miocene unconformity were largely folded and faulted (Kugler, 1959; Speed, 1985; and Soto et al., 2011). In the Southern Basin, Babb and Mann (1999) identified a few compressional structures but noticed that generally they only correspond to subtle middle Miocene folding and faulting.

In the lower middle Miocene Guaracara limestone (Tamana Formation), we found strike-slip faults that predate the middle Miocene unconformity (Figure 8). The trend of compression (east-northeast–west-southwest) is not consistent with the right-lateral strike-slip motion on the southern Caribbean margin. We propose that the mesoscale faults, indicating this trend of compression, have been rotated clockwise via block rotation. The observed strike-slip faults suggest that slip on larger strike-slip faults may have resulted in large (~90°) clockwise block rotations about vertical axis during the passage of the edge of the Caribbean plate along the South America passive margin (Figure 16A).

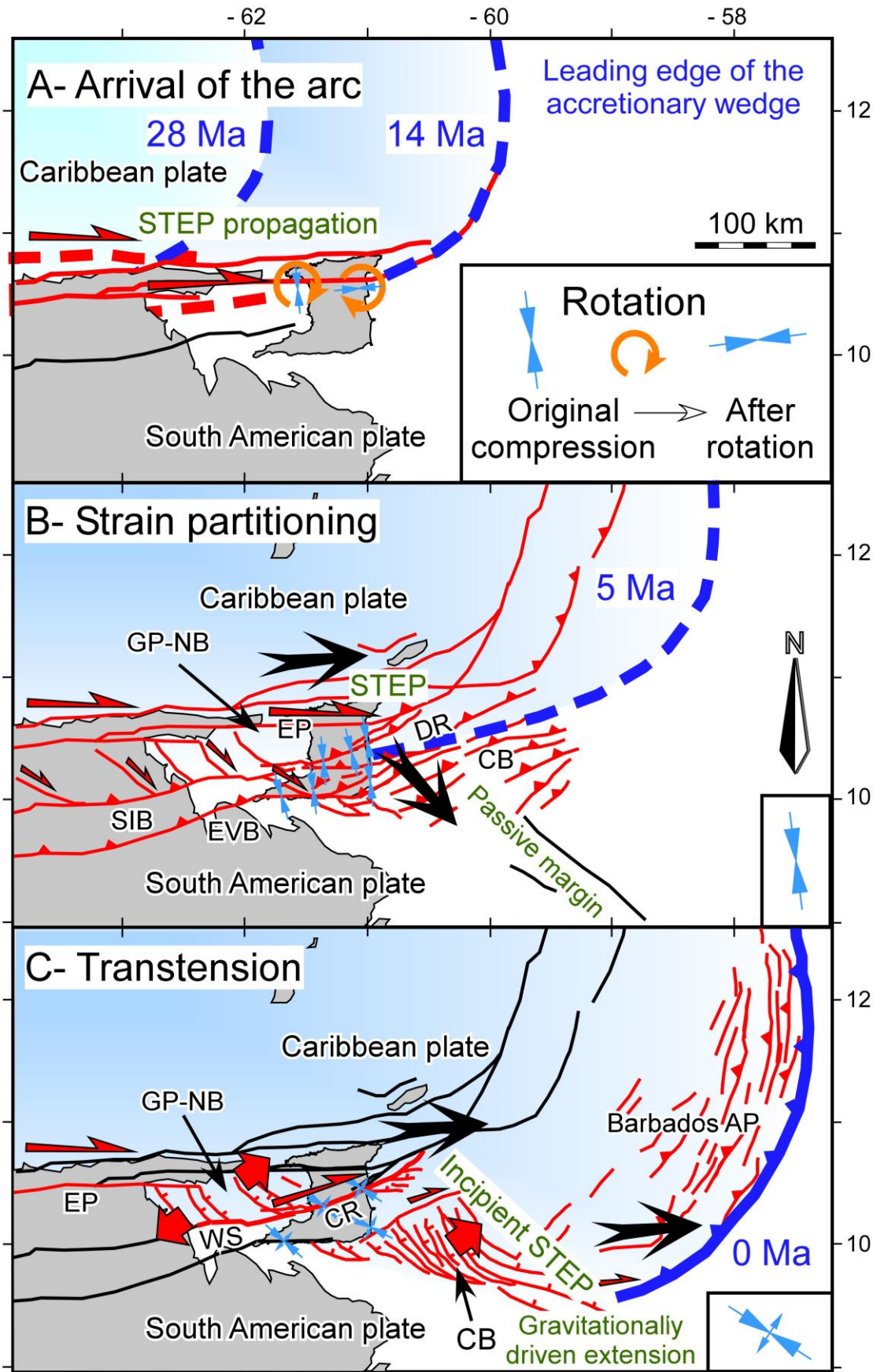


Figure 16. Proposed, three-stage model for the southeastern Caribbean based on the fault data presented in this chapter. (A) Middle Miocene oblique collision and block rotation as the Caribbean plate and the Great Arc of the Caribbean move eastward along the South American passive margin of Venezuela and Trinidad. The successive positions of the leading edge of the Caribbean plate, based on ages of foreland basin deposits are from Escalona and Mann (2011) and Garciacaro et al. (2011). Clockwise rotations are consistent with a model of eastward propagation of the Subduction-Transform Edge Propagator (STEP); Govers and Wortel, 2005) and with models of right-lateral strike-slip faults rotating either fault blocks or a structural coherent mass. (B) Late Miocene–middle Pliocene strain partitioning between large right-lateral strike-slip faults bounding the Great Arc of the Caribbean, and fold–thrust belts along the northern margin of the South American plate. (C) Late Pliocene–Quaternary transtension characterized in Trinidad by extensional and strike-slip faulting. Transtensional deformation can be interpreted as the surface expression of an incipient southeastward propagation of the lateral slab tear fault (“STEP” fault) along the south–east-trending continent–ocean boundary between the South American passive margin and the subducting oceanic plate of the Atlantic Ocean. CB = Columbus Basin; AP = Accretionary prism; CR = Central Range fault zone; DR = Darien ridge; EP = El Pilar fault zone, EVB = eastern Venezuela Foreland Basin; GP–NB = Gulf of Paria–Northern basin; SIB = Serranía del Interior belt; WS = Warm Springs fault zone; STEP = Subduction-Transform Edge Propagator. Large black arrows show possible displacement directions. Harpoon red arrows indicate strike-slip displacements. Thick red arrows show extension. Little blue double arrows show the trends of compression or extension determined in this chapter.

Block rotations may be common at the lateral edges of subduction zones characterized by trench rollback. Govers and Wortel (2005) showed that continued subduction requires tearing of the lithosphere near terminations of subduction trenches and named such features as Subduction-Transform Edge Propagators (STEPS). During STEP propagation, relative horizontal motion across the STEP faults might result in substantial deformation and rotations about vertical axes. Govers and Wortel (2005) proposed that the Lesser Antilles trench, like the Carpathian and Calabrian subduction zones, is laterally bounded by STEP-fault zones at its northern and southern ends. The eastward propagation of the STEPs may have produced counterclockwise rotations along the northern Caribbean plate boundary and clockwise rotations along the South America continental margin. Consequently, our model of clockwise block rotations in Trinidad during the middle Miocene is consistent with the clockwise rotations about vertical axis expected along the right-lateral STEP fault that has propagated along the passive continental margin of South America and has crossed Trinidad during the early middle Miocene (Figure 16A).

VI-2- Late Miocene to Middle Pliocene Collision and Strain Partitioning

The late Neogene deformation along the southeastern Caribbean margin is characterized by strike-slip faults and south verging thrusts, and is transpressional (Figure 16B). In Venezuela, the Serranía del Interior belt is characterized by south to southeast-vergent thrusting that occurred in Oligocene through Pliocene (Roure et al., 1995). The Morochito piggyback basin was filled during the late Miocene and Pliocene (Roure et al., 1995; Babb and Mann, 1999).

In Trinidad, along strike of the Serranía del Interior belt, the upper Miocene and Pliocene sediments of the Southern basins are involved in south-vergent thrusting and folding (Figure 16B). The Central Range of Trinidad was also structurally uplifted during the late Miocene–early Pliocene as shown by offshore deposits of conglomerates (Babb and Mann, 1999). The fold–thrust belt that was formed in southern Trinidad is characterized by south–southeast-trending compression (Figure 9). The right-lateral slip along the Los Bajos oblique ramp, which terminates into thrusting along the Southern Range, occurred under this stress field. However, the largest right-lateral strike-slip faults were at the rear of the fold–thrust belt and strike east–west along the Northern Range (Figure 16B).

Fission track ages by Algar and Pindell (1993) from rocks of the Northern Range indicate that shallow unroofing and erosion began early late Miocene, ca. 11 Ma ago. A more recent study gives ages for shallow exhumation from ca. 15 Ma to ca. 4 Ma (Denison et al., 2008). These ages are consistent with stratigraphic data. Babb and Mann (1999) interpret upper Miocene coarse siliciclastic sedimentation in the Gulf of Paria and Northern Basin related to erosion of the Northern Range as the first manifestation of down to the south oblique slip motions on the El Pilar fault zone. The conglomerate of the Cunapo Formation, forms a several-kilometer (several thousands of feet)-thick siliciclastic wedge interpreted as a foreland basin wedge (Elling et al., 2019). This conglomerate interfingers with sandstone of the Manzanilla Formation, thus giving the Cunapo Formation a late Miocene to early Pliocene age and a similar age to the activity of the El Pilar fault zone (Babb and Mann, 1999).

The late Miocene to middle Pliocene south-southeast-trending compression is consistent with the right-lateral motion along the El Pilar fault zone during this period. We infer from the deformation pattern of Figure 16B, and from the south-southeast-trending compression, that transpressional deformation at this time along the south Caribbean margin was resolved by strain partitioning (Figures 1, 16B). Southeastward displacements along the south Caribbean margin was partitioned into an arc-subnormal component in the outer fold-thrust belts like in the Southern Basin and the Southern Range for Trinidad and an arc-parallel strike-slip motion along the internal El Pilar fault zone (Figure 16B). Note that strain partitioning is frequent in an oblique collisional context and in the Caribbean arc it was previously proposed for present deformation occurring in Venezuela based on the analysis of fault-slip data (Audemard et al., 2005) and in Hispaniola based on present strain accumulation rates on regional faults (Calais et al., 2002).

During the late Miocene, the strike-slip Central Range fault was not yet active. But in the middle and late Pliocene, the Gulf of Paria basin began opening as a pull-apart basin generated by the gradual transfer of slip from the Trinidadian El Pilar fault zone to the Warm Springs and Central Range fault zones (Babb and Mann, 1999). We have no sites in Pliocene rocks along the Central Range to date accurately the end of the south-southeast-trending compression and the activation of the Central Range fault. However, site Erin3 and the right-lateral offset of Pliocene rocks of the Erin Formation by the Los Bajos fault indicate that in southern Trinidad compression may have remained oriented north-northwest-south-southeast until the late Pliocene.

VI-3- Late Pliocene-Pleistocene Transtension as a Response to Southeastward Propagation of the Subduction Front

During the Pliocene, most of right-lateral slips in Trinidad shifted to the Warm Springs-Central Range zone (Figure 16C; Babb and Mann, 1999). A pull-apart basin formed at the stepover area between the Venezuelan El Pilar Fault and the Warm Springs fault zone in the Gulf of Paria (Figure 12). Formation of the stepover may have deactivated slip along the eastern continuation of the El Pilar fault zone along the northern margin of the Northern Basin (Speed, 1985; Babb and Mann, 1999).

Pindell et al. (2005) also proposed that a tectonic change occurred at ca. 4 Ma, based on enhanced rates of pull-apart formation in the Gulf of Paria and initiation of extensional collapse of the foredeep basin fill toward the Atlantic south of the Darien Ridge (Wood, 2000). In Trinidad, we show that stress field changed from south-southeast-trending late Miocene-middle Pliocene compression, consistent with the right-lateral slip along the El Pilar fault zone in northern Trinidad, to a more recent east-northeast-trending compression, compatible with the right-lateral

slip on the Central Range fault. In northern and western Venezuela, however, Quaternary compression is still trending north-northwest–south-southeast, and strain is still partitioned between right-lateral east–west trending strike-slip faults and east-northeast-trending thrusts and folds (Audemard et al., 2005).

The recent stress field in Trinidad not only rotated but also changed to mainly strike-slip regime characterized by stress permutations to extension, as it was frequently shown in the field by small normal faults (Figure 12). At the scale of the island of Trinidad, while the Central Range fault zone was characterized by transpression, we can note that normal faulting occurred offshore along east–west to northwest–southeast faults in the Gulf of Paria (Babb and Mann, 1999), in the Columbus Basin (Wood, 2000), and immediately south of the eastern offshore extension of the Central Range strike-slip fault system (Soto et al., 2011). Hence, the Pliocene evolution of the stress field was not simply a rotation of the trends of compression but reflects a major structural change along the southeastern Caribbean margin.

Without improved paleomagnetic data, we cannot rule out the idea that Trinidad was rotated clockwise during the late Neogene to explain the differences in stress orientations between Phases 2 and 3 (Figures 9, 12). However, this hypothetical recent rotation should be limited because the El Pilar fault has the same trend in Trinidad and in Venezuela. Furthermore, paleomagnetism data showed no rotation of mid-Pliocene rocks in the neighboring Tobago Island (Weber et al., 2014). Paleostress and structural data suggest instead that the evolution from Phase 2 to Phase 3 reflects a major geodynamic change.

Given that stress permutations to extensional regime generally denote a diminution of lateral confining pressure (Hippolyte et al., 1992), we think that the change from transpressional to transtensional deformation in Trinidad area was related to a change in the boundary conditions along the South American passive margin. A major structural change that occurred since the late Miocene is the southeastward propagation of the leading edge of the Barbados accretionary prism (Figure 16B, C). The accretionary prism has extended to the southeast along the southeast-striking South American passive margin (Figure 16C). Another change is the thick accumulation of sediments from the Orinoco River on the South American margin. But a major geodynamic change that may have occurred in this area is the propagation along the South American continental margin of the southern STEP fault of the Caribbean subduction (Govers and Wortel, 2005).

Therefore, diminution of the eastward confining stresses might result either from vertical flexure of the South American Margin under the weight of the Barbados prism, or sediments of the Orinoco River, or as a consequence of slab pull forces and STEP propagation. The Pliocene structural reorganization at the southeastern Caribbean margin could be the surface tectonic expression of the prelude for STEP propagation. Because the direction of the STEP propagation generally follows weakness zones such as continental passive margins (Govers and Wortel, 2005), it will probably follow the change of strike of the South American passive margin that is trending northwest–southeast immediately east of Trinidad (Figure 16B). Whatever the model is, it is notable that extensional deformation occurs in the areas south of the El Pilar fault zone where possible east-directed tractions are less compensated by the eastward drift of the Caribbean plate.

VII- CONCLUSIONS

Fault kinematic analysis and paleostress reconstructions document three major tectonic stages in the Neogene through Holocene tectonic evolution of Trinidad. The three tectonic stages we propose are consistent with the structural evolution of Trinidad and the basins around Trinidad known from previous workers such as Babb and Mann (1999), Garciacaro et al. (2011), and Escalona and Mann (2011).

(1) During Stage 1, a middle Miocene shortening event was mainly recognized based on a widespread middle Miocene, angular unconformity. Our discovery of faults affecting the Central Range area before the middle Miocene unconformity at ca. 12 Ma confirms that this unconformity is tectonically significant because the stress pattern changes in rocks overlying the unconformity. Fault slip data indicate that the middle Miocene deformation was mainly strike-slip faulting with σ_1 axis presently oriented east-northeast–west-southwest (Figure 7). This trend of compression and the observed strike-slip faulting suggest that large-scale rotations have occurred in Trinidad at the arrival of the Caribbean arc.

(2) The late Miocene–middle Pliocene stress field was characterized by a north-northwest–south-southeast trend of compression. This compressional event resulted in folding and south-verging thrusts from the Central Range to the Southern Range. We interpret oblique faults, including the Los Bajos fault, as either right-lateral ramps or left lateral ramps, of mainly south-southeast-vergent thrusts. A southward-fining and thinning siliciclastic wedge derived from the Central range supports the activity of the El-Pilar strike-slip fault in particular during the late Miocene–early Pliocene (Babb and Mann, 1999). The stress field of central and southern Trinidad is consistent with the right-lateral motion along this fault and other parallel strike-slip faults of northern Trinidad. We infer that strain partitioning characterizes the late Miocene–middle Pliocene deformation of Trinidad.

(3) The most recent deformation in Trinidad is strike-slip faulting, with minor stress permutations manifested by localized areas of perpendicular extension. We characterized this deformation mainly along the Central Range fault that accommodates 70% of the total Caribbean–South America plate motion in Trinidad (Weber et al., 2001a). The trend of compression rotated to west-northwest–east-southeast. We link this change of compression trend to the activation of the Central Range fault as strike-slip fault and to the end of slip along the El Pilar fault zone in Trinidad, and probably also along the Los Bajos fault and the thrusts of southern Trinidad. We also identified this recent compression in southern Trinidad. Its onset age could be correlated either to the beginning or to the end of deposition of the Erin Formation, that is, late Pliocene or early Pleistocene. Stress permutation to extension in Trinidad seems to be linked to extensional deformation occurring offshore in the Gulf of Paria pull-apart basin.

The evolution of the paleostress regimes is interpreted as a consequence of the eastward motion of the Caribbean arc along Trinidad, and the propagation of the southern STEP fault of the Caribbean subduction. Reconstruction of paleostresses provided critical information about the kinematics and timing of deformation that was used for understanding plate tectonic interactions and evolution.

ACKNOWLEDGMENTS

We thank the organizers and members of the Geological Society of Trinidad and Tobago for their informative conferences and conference-related, field trips that helped guide our field studies and place stratigraphic and age constraints on the faulted strata we studied in Trinidad. The authors thank the industry sponsors of the Caribbean Basins and Tectonics (CBT) consortium for their financial support of fieldwork in Trinidad. Finally, we are grateful to John Weber for his assistance with field work in Trinidad, and Catherine Homberg, Claudio Bartolini, and John Weber for their constructive reviews of this chapter.

REFERENCES

- Aitken, T., P. Mann, A. Escalona, and G. L. Christeson, 2011, Evolution of the Grenada and Tobago basins and implications for arc migration: *Marine and Petroleum Geology*, v. 28, p. 235–258, doi:10.1016/j.marpetgeo.2009.10.003.
- Algar, S. T., and J. Pindell, 1993, Structure and deformation history of the Northern Range of Trinidad and adjacent areas: *Tectonics*, v. 12, p. 814–829.
- Alvarez, T., P. Mann, and L. Wood, 2019, Tectonics and the evolution of sedimentary basins along the arcuate southeastern margin of the Caribbean plate, *in* C. Bartolini, ed., *Eastern Caribbean–northeastern South American boundary: Tectonic evolution, basin architecture, and petroleum systems: AAPG Memoir XXX*, p. XX–XX.
- Anderson, E. M., 1951, *The dynamics of faulting and dyke formation with applications to Britain*, 2nd ed.: Edinburgh, Scotland, Oliver and Boyd, 206 p.
- Angelier, J. 1990, Inversion of field data in fault tectonics to obtain the regional stress: A new rapid direct inversion method by analytical means: *Geophysical Journal International*, v. 103, p. 363–376.
- Angelier, J. 1994, Fault slip analysis and palaeostress reconstruction, *in* P. L. Hancock, ed., *Continental Deformation: Oxford, U.K., Pergamon Press*, p. 53–100.
- Angelier, J., A. Tarantola, B. Valette, and S. Manoussis, 1982, Inversion of field data in fault tectonics to obtain the regional stress, I, Single phase fault populations: A new method of computing the stress tensor: *Geophysical Journal of the Royal Astronomical Society*, v. 69, p. 607–621.
- Audemard, F. A., 2001, Quaternary tectonics and present stress tensor of the inverted northern Falcon Basin, northwestern Venezuela: *Journal of Structural Geology*, v. 23, p. 431–453.
- Audemard, F. A., G. Romero, H. Rendon, and V. Cano, 2005, Quaternary fault kinematics and stress tensors along the southern Caribbean from fault-slip data and focal mechanism solutions: *Earth-Science Reviews*, v. 69, p. 181–233.
- Avé Lallemant, H. G., 1997, Transpression, displacement partitioning, and exhumation in the eastern Caribbean/South American plate boundary zone: *Tectonics*, v. 16, p. 272–289.
- Babb, S., and P. Mann, 1999, Structural and sedimentary development of a Neogene transpressional plate boundary between the Caribbean and South America plates in Trinidad and the Gulf of Paria, *in* P. Mann, *Caribbean basins: Elsevier Sedimentary Basins of the World 4*, p. 495–557.
- Beardsley, A. G., and H. G. Avé Lallemant, 2007, Oblique collision and accretion of the Netherlands Leeward Antilles to South America: *Tectonics*, v. 26, p. TC2009, doi: 10.1029/2006TC002028.
- Bolli, H. M., J. P. Beckmann, and J. B. Saunders, 1995, *Benthic foraminiferal biostratigraphy of the south Caribbean region*: Cambridge, U.K., Cambridge University Press, 408 p.
- Bowman, A. P., and H. D. Johnson, 2014, Storm-dominated shelf-edge delta successions in a high accommodation setting: The palaeo-Orinoco Delta (Mayaro Formation), Columbus Basin, South-East Trinidad: *Sedimentology*, v. 61, p. 792–835.
- Burke, K., 1988, Tectonic evolution of the Caribbean: *Annual Review of Earth and Planetary Sciences*, v. 16, p. 201–230.

- Burmester, R. F., M. E. Beck, R. C. Speed, and A. W. Snoke, 1996, A preliminary paleomagnetic pole for mid-Cretaceous rocks from Tobago: Further evidence for large clockwise rotations in the Caribbean–South American plate boundary zone: *Earth and Planetary Science Letters*, v. 139, p. 79–90.
- Calais, E., Y. Mazabraud, B. M. de Lépinay, P. Mann, G. Mattioli, and P. Jansma, 2002, Strain partitioning and fault slip rates in the northeastern Caribbean from GPS measurements: *Geophysical Research Letters*, v. 29, no. 18, p. 1856, doi: 10.1029/2002GL015397.
- Carey, E., and B. Brunier, 1974, Analyse théorique et numérique d'un modèle mécanique élémentaire appliqué à l'étude d'une population de failles: *Comptes-Rendus Académie des Sciences, Paris*, v. 279, p. 891–894.
- Célérier, B., A. Etchecopar, F. Bergerat, P. Vergely, F. Arthaud, and P. Laurent, 2012, Inferring stress from faulting: From early concepts to inverse methods: *Tectonophysics*, v. 581, p. 206–219.
- Christenson, G. L., P. Mann, A. Escalona, and J. A. Trevor, 2008, Crustal structure of the Caribbean–northeastern South America arc-continent collision zone: *Journal of Geophysical Research*, v. 113, 19 p., doi: 10.1029/2007JB005373.
- De Verteuil, L., B. Ramlal, and J. Weber, 2006, *Trinidad Geological GIS, Module 1: Surface Geology and Geography: Port of Spain, Trinidad and Tobago*, Latinum, Ltd.
- Denison, C., J. Weber, R. Donelick, and P. O'Sullivan, 2008, Apatite fission-track thermochronology, northern range, Trinidad (and Paria Peninsula, Venezuela), Ph.D. thesis, Grand Valley State University, Allendale, Michigan, 39 p.
- Deville, E., A. Mascle, Y. Callec, P. Huyghe, S. Lallemand, O. Lerat, X. Mathieu et al., 2015, Tectonics and sedimentation interactions in the east Caribbean subduction zone: An overview from the Orinoco delta and the Barbados accretionary prism: *Marine and Petroleum Geology*, v. 64, p. 76–103.
- Díaz de Gamero, M., 1996, The changing course of the Orinoco River during the Neogene: A review: *Palaeogeography, Palaeoclimatology, Palaeoecology*, v. 123, no. 1–4, p. 385–402.
- Elling, R., P. Farfan, and J. Weber, Cunapo conglomerate, Northern Basin and Central Range, Trinidad: Neogene syn-contractile tectonic marker unit - Field and petrographic study, *in* C. Bartolini, ed., *Eastern Caribbean–northeastern South American boundary: Tectonic evolution, basin architecture, and petroleum systems: AAPG Memoir 123*, p. 695–712.
- Erlich, R., P. Farfan, and P. Hallock, 1993, Biostratigraphy, depositional environments, and diagenesis of the Tamana Formation, Trinidad: A tectonic marker horizon: *Sedimentology*, v. 40, p. 743–768.
- Escalona, A., and P. Mann, 2011, Tectonics, basin subsidence mechanisms, and paleogeography of the Caribbean–South American plate boundary zone: *Marine and Petroleum Geology*, v. 28, p. 8–39.
- Frey, M., J. Saunders, and H. Schwander, 1988, The mineralogy and metamorphic geology of low-grade metasediments, Northern Range, Trinidad: *Journal of the Geological Society of London*, v. 145, p. 563–575.
- Garciacaro, E., P. Mann, and A. Escalona, 2011, Regional structure and tectonic history of the obliquely colliding Columbus foreland basin, offshore Trinidad and Venezuela: *Marine and Petroleum Geology*, v. 28, no. 1, p. 126–148.
- Giorgis, S., J. Tong, and R. Sirianni, 2009, Constraining neotectonic orogenesis using an isostatically compensated model of transpression: *Journal of Structural Geology*, v. 31, p. 1074–1083.
- Giorgis, S., J. Weber, A. M. Glose, M. Ward, B. Hocking, and K. Sharman, 2008, Paleomagnetic constraints on shortening across the Central Range fault zone, Trinidad (abs.): *Geological Society of America Annual Meeting, Houston, Texas, October 5–9, 2008*.
- Giorgis, S., J. Weber, J. Hojnowski, W. Pierce, and A. Rodriguez, 2011, Using orthographic projection with geographic information system (GIS) data to constrain the kinematics the Central Range fault zone, Trinidad: *Journal of Structural Geology*, v. 33, p. 1254–1264, doi: 10.1016/j.jsg.2011.05.008.
- Giorgis, S., J. Weber, S. Sanguinito, C. Beno, and J. Metcalf, 2017, Thermochronology constrains on Miocene exhumation in the Central Range Mountains, Trinidad: *GSA Bulletin*, v. 129, p. 171–178, doi: 10.1130/B31363.1.
- Gomez, S., D. Bird, and P. Mann, 2018, Deep crustal structure and tectonic origin of the Tobago-Barbados ridge: *Interpretation*, v. 6, no. 2, p. T471–T484, doi: 10.1190/INT-2016-0176.1.

- Govers, R., and M. J. R. Wortel, 2005, Lithosphere tearing at STEP faults: Response to edges of subduction zones: *Earth and Planetary Science Letters*, v. 236, p. 505–523.
- Hippolyte, J. C., J. Angelier, and F. Roure, 1992, Les permutations de contraintes dans un orogène: exemple des terrains quaternaires du sud de l'Apennin: *Comptes rendus de l'Académie des Sciences, Paris*, v. 315, Série II, p. 89–95.
- Hippolyte, J. C., F. Bergerat, M. B. Gordon, O. Bellier, and N. Espurt, 2012, Keys and pitfalls in mesoscale fault analysis and paleostress reconstructions, the use of Angelier's methods: *Tectonophysics*, v. 581, p. 144–162, doi: 10.1016/j.tecto.2012.01.012.
- Hippolyte, J.-C., and M. Sandulescu, 1996, Paleostress characterization of the 'Wallachian phase' in its type area (southeastern Carpathians, Romania): *Tectonophysics*, v. 263, p. 235–248, doi:10.1016/S0040-1951(96)00041-8
- Homberg, C., J. Schnyder, and M. Benzaggagh, 2013, Late Jurassic–Early Cretaceous faulting in the Southeastern French basin: Does it reflect a tectonic reorganization?: *Bulletin de la Société géologique de France*, v. 184, no. 4–5, p. 501–514.
- Jouanne, F., F. A. Audemard, C. Beck, A. Van Welden, R. Ollarves, and C. Reinoza, 2011, Present-day deformation along the El Pilar Fault in eastern Venezuela: Evidence of creep along a major transform boundary: *Journal of Geodynamics*, v. 51, p. 398–410.
- Kugler, H., 1959. Geological Map of Trinidad and Geological Section through Trinidad: Port of Spain, Trinidad and Tobago, The Petroleum Association of Trinidad, scale 1:100,000.
- Kugler, H. G., 1953, Jurassic to Recent sedimentary environments in Trinidad: *Bulletin de l'Association Suisse des Géologues et Ingénieurs du Pétrole*, v. 20, no. 59, p. 27–60.
- Kugler, H. G., 2001, *Treatise on the Geology of Trinidad. Part 4: Paleocene to Holocene Formations*: Basel, Switzerland, Natural History Museum of Basel, 309 p.
- MacDonald, W. D., 1980, Net Tectonic rotation, apparent tectonic rotation, and the structural tilt correction in paleomagnetic studies: *Journal of Geophysical Research*, v. 85, no. B7, p. 3659–3669.
- Mann, P., C. Schubert, and K. Burke, 1990, Review of Caribbean neotectonics, *in* G. Dengo and J. E. Case, eds., *The Caribbean region: GSA The Geology of North America H*, p. 307–338.
- Nelson, M. R., and C. H. Jones, 1987, Paleomagnetism and crustal rotations along a shear zone, Las Vegas Range, Southern Nevada: *Tectonics*, v. 6, no. 1, p. 13–33.
- Payne, N., 1991, An evaluation of post-middle Miocene geological sequences, offshore Trinidad: *Transactions of the Geological Conference of the Geological Society of Trinidad & Tobago*, v. 2, p. 70–87.
- Pérez, O. J., and Y. P. Aggarwal, 1981, Present-day tectonics of the southeastern Caribbean and northeastern Venezuela: *Journal of Geophysical Research*, v. 86, p. 10791–10804.
- Pérez, O. J., R. Bilham, R. Bendick, J. R. Velandia, N. Hernández, C. Moncayo, M. Hoyer, and M. Kozuch, 2001, Velocity field across the southern Caribbean plate boundary and estimates of Caribbean/South American plate motion using GPS geodesy 1994–2000: *Geophysical Research Letters*, v. 28, p. 2987–2990, doi: 10.1029 /2001GL013183.
- Persad, K. M., 1984, *Geologic-Tectonic map of Trinidad and Tobago*: Houston, Texas, Robertson Research (U.S.) Inc., scale 1:200,000.
- Pindell, J. L., and S. F. Barrett, 1990, Geological evolution of the Caribbean region: A plate tectonic perspective, *in* G. Dengo and J. E. Case, eds., *The Caribbean region: GSA Geology of North America H*, p. 405–432.
- Pindell, J. L., R. Higgs, and J. F. Dewey, 1998, Cenozoic palinspastic reconstruction, paleogeographic evolution and hydrocarbon setting of the northern margin of South America, *in* J. L. Pindell and C. Drake, eds., *Paleogeographic evolution and non-glacial eustasy, Northern South America: SEPM Special Publication 58*, p. 45–85.
- Pindell, J. L., and L. Kennan, 2001, Processes & events in the terrane assembly of Trinidad and E. Venezuela, *in* GCSSEPM Foundation 21st Annual Research Conference Transactions, Petroleum Systems of Deep-Water Basins, December 2–5, 2001, Houston, Texas, p. 159–192.
- Pindell, J. L., L. Kennan, W. V. Maresch, K. P. Stanek, G. Draper, and R. Higgs, 2005, Plate-kinematics and crustal dynamics of circum-Caribbean arc-continent interactions: Tectonic controls on basin development in

- proto-Caribbean margins, in H. G. Ave Lallemand and V. B. Sisson, Caribbean-South American plate interactions: GSA Special Paper 394, p. 7–52, doi: 10.1130/0-8137-2394-9.7.
- Prentice, C., J. Weber, C. Crosby, and D. Ragona, 2010, Prehistoric earthquakes on the Caribbean–South American plate boundary, Central Range fault, Trinidad: *Geology*, v. 38, no. 8, p. 675–678, doi: 10.1130/G30927.1.
- Reinoza, C., F. Jouanne, F. A. Audemard, M. Schmitz, and C. Beck, 2015, Geodetic exploration of strain along the El Pilar Fault in northeastern Venezuela: *Journal of Geophysical Research: Solid Earth*, v. 120, p. 1993–2013, doi: 10.1002/2014JB011483.
- Robertson, P., and K. Burke, 1989, Evolution of southern Caribbean plate boundary, vicinity of Trinidad and Tobago: *AAPG Bulletin*, v. 73, p. 490–509.
- Roure, F., J. O. Carnevali, Y. Gou, and T. Subicta, 1995, Geometry and kinematics of the North Monagas thrust belt (Venezuela): *Marine and Petroleum Geology*, v. 11, p. 347–362.
- Russo, R. M., and R. C. Speed, 1992, Oblique collision and tectonic wedging of the South American continent and Caribbean terranes: *Geology*, v. 20, p. 447–450.
- Sandwell, D. T., and W. H. F. Smith, 2009, Global marine gravity from retracked Geosat and ERS-1 altimetry; ridge segmentation versus spreading rate: *Journal of Geophysical Research*, v. 114, p. B01411
- Saunders, J. B., 1998, Geological map of Trinidad and Tobago: Port of Spain, Trinidad and Tobago, Ministry of Energy and Energy Industries (TTMEEI), scale: 1:100,000.
- Skerlec, G. M., and R. B. Hargraves, 1980, Tectonic significance of paleomagnetic data from northern Venezuela: *Journal of Geophysical Research*, v. 85, no. B10, p. 5303–5315.
- Soto, D., P. Mann, and A. Escalona, 2011, Miocene-to-recent structure and basinal architecture along the Central Range strike-slip fault zone, eastern offshore Trinidad: *Marine and Petroleum Geology*, v. 28, p. 212–234.
- Speed, R. C., 1985, Cenozoic collision of the Lesser Antilles arc and continental South America and the origin of the El Pilar fault: *Tectonics*, v. 4, p. 41–69, doi: 10.1029/TC004i001p00041.
- Stearns, C., F. Mauk, and R. Van der Voo, 1982, Late Cretaceous–Early Tertiary paleomagnetism of Aruba and Bonaire (Netherlands Leeward Antilles): *Journal of Geophysical Research*, v. 87, p. 1127–1141.
- Symithe, S., E. Calais, J. B. de Chabaliere, R. Robertson, and M. Higgins, 2015, Current block motions and strain accumulation on active faults in the Caribbean: *Journal of Geophysical Research: Solid Earth*, v.120, p. 3748–3774, doi: 10.1002/2014JB011779.
- Weber, J., J. Arkle, S. Giorgis, and J. C. Hippolyte, 2014, New thermochronologic, paleomagnetic, and fault-slip constraints on Pliocene Tectonics and provenance, North Coast Marine area, Trinidad and Tobago: AAPG meeting (workshop) March 2014, Trinidad.
- Weber, J., T. H. Dixon, C. DeMets, W. B. Ambeh, P. Jansma, G. Mattioli, J. Saleh, G. Sella, R. Bilham, and O. Pérez, 2001a, GPS estimate of relative motion between the Caribbean and South American plates, and geological implications for Trinidad and Venezuela: *Geology*, v. 29, p. 75–78.
- Weber, J. C., D. Ferrill, and M. Roden-Tice, 2001b, Calcite and quartz microstructural geothermometry of low-grade metasedimentary rocks, Northern Range, Trinidad: *Journal of Structural Geology*, v. 23, p. 93–112.
- Weber, J., J. Saleh, S. Balkaransingh, T. Dixon, W. Ambeh, T. Leong, A. Rodriguez, and K. Miller, 2011, Triangulation-to-GPS and GPS-to-GPS geodesy in Trinidad, West Indies: Neotectonics, seismic risk, and geologic implications: *Journal of Petroleum and Marine Geology*, v. 28, p. 200–211, doi: 10.1016/j.marpetgeo.2009.07.010.
- Wharton, S., A. Dupigny, and J. Keens-Dumas, 1986, A preliminary investigation of the Brigand Hill Limestone, Brigand Hill Quarry, Plum Mitán Road, in K. Rodrigues, ed., Transactions of the First Geological Conference of The Geological Society of Trinidad and Tobago: Port of Spain, Trinidad and Tobago, July 10–12, 1985, p. 102–113.
- Wilson, B., 2007, Benthonic foraminiferal palaeoecology of the Brasso Formation (*Globorotalia fohsi lobata* and *Globorotalia fohsi robusta* (N11–N12) Zones, Trinidad, West Indies: A transect through an oxygen minimum zone: *Journal of South American Earth Sciences*, v. 23, p. 91–98.

- Wilson, B., 2012, Planktonic Foraminifera in the Early to Middle Miocene 'Lower Concord Calcareous Silt Member' at Mayo Quarry, Central Trinidad, and the invalidity of the Tamana Formation: *Newsletters on Stratigraphy*, v. 45, p. 105–114.
- Wilson, B., 2013, Foraminiferal biofacies in the san Jose calcareous silt member (Manzanilla Formation, upper Miocene to lower Pliocene) in the Manzanilla bay area, north-east Trinidad, and their environmental significance: *Journal of South American Earth Sciences*, v. 46, p. 80–88.
- Wilson, B., P. Farfan, and C. Hughes, 2017, The formation placement and palaeoenvironment of the Middle Miocene Los Atajos Member, Trinidad: *Journal of South American Earth Sciences*, v. 76, p. 63–70, doi: 10.1016/j.jsames.2017.02.013.
- Wilson, B., B. Jones, and K. Birjue, 2010, Palaeoenvironmental interpretations based on foraminiferal abundance biozones, Mayo Limestone, Trinidad, West Indies, including alpha and beta diversities: *Palaeos*, v. 25, p. 158–166. doi: 10.2110/palo.2009.p09-118r.
- Wilson, B., M. Ramkissoo, and A. McLean, 2011, The biostratigraphic and palaeoenvironmental significance of foraminifera in the Middle Miocene Upper Concord Calcareous Silt Member (Tamana formation) near Gasparillo West Quarry, central Trinidad: *Cainozoic Research*, v. 8, p. 3–12.
- Wilson, C. C., 1940, The Los Bajos fault of south Trinidad, BWI: *AAPG Bulletin*, v. 24, p. 2102–2125.
- Wood, L., 2000, Chronostratigraphy and tectonostratigraphy of the Columbus Basin, eastern 13 offshore Trinidad: *AAPG Bulletin*, v. 84, no. 12, p. 1905–1928.

Table 1. Latitudes and Longitudes of the 20 Mesoscale, Fault Sites and their Computed Paleostresses. The formation names and the age of rocks are from Saunders (1998) and De Verteuil et al. (2006). **Abbreviations:** (1) Stress regimes: C = compressional; S = strike-slip; E = extensional; SC = strike-slip and compressional; (2) σ_1 , σ_2 and σ_3 = maximum, intermediate, and minimum principal stress axis, respectively; (3) tr., pl. = trend (north to east) and plunge in degrees ($^\circ$) of the stress axes; (4) ratio $\Phi = (\sigma_2 - \sigma_3)/(\sigma_1 - \sigma_3)$; (5) ANG = average angle between computed shear stress and observed slickenside lineation ($^\circ$); (6) RUP = quality estimator ($0 \leq RUP \leq 200$) taking into account the relative magnitude of the shear stress on fault planes (cf. Angelier, 1990).

Site name	Latitude	Longitude	easting UTM 20	northing UTM 20	formation or member	age of rocks	stress regime	number of faults	σ_1 tr.	σ_1 pl.	σ_2 tr.	σ_2 pl.	σ_3 tr.	σ_3 pl.	Φ	ANG	RUP
FORTIN1	10.155600	-61.725883	639581	1122890	Erin	Upper Pliocene	E	9	180	83	327	6	58	4	0.26	11	25
FORTIN2	10.148433	-61.787867	632791	1122069	Erin	Upper Pliocene	SC	12	279	2	185	64	10	26	0.16	15	43
ERIN1	10.083950	-61.688383	643721	1114983	Erin	Upper Pliocene	C	11	312	9	43	8	173	78	0.32	9	29
ERIN2	10.082467	-61.686017	643982	1114819	Erin	Upper Pliocene	E	14	144	72	321	18	51	1	0.34	11	24
ERIN3	10.085917	-61.707817	641593	1115192	Erin	Upper Pliocene	S	4	344	34	200	50	87	18	0.65	4	19
PENAL	10.133067	-61.453767	669413	1120528	Morne l'Enfer	Pliocene	S	6	353	9	143	80	262	5	0.45	3	16
MAYARO1	10.190167	-61.001783	718924	1127009	Mayaro sand	Pliocene	S	14	297	3	201	58	29	32	0.19	15	41
			718907	1127114			SC	10	174	11	71	48	273	39	0.05	17	41
MAYARO2	10.167817	-60.998717	719261	1124634	Mayaro sand	Pliocene	E	15	180	86	88	0	358	4	0.44	9	33
MAYARO3	10.155300	-61.002310	718875	1123256	Mayaro sand	Pliocene	E	3									
MAYARO4	10.135567	-61.061667	712383	1121035	Moruga Fm (G. Morne)	Upper Miocene	S	12	164	42	339	48	72	2	0.12	10	42
P. RADIX	10.330167	-60.971050	722179	1142623	Moruga Fm (Trin. Hill)	Upper Miocene	E	19	307	69	66	11	159	18	0.46	10	27
							S	12	161	28	0	60	255	9	0.49	16	58
P. MANZA	10.515633	-61.029417	715657	1163101	Guaracara ? San Jose ?	Miocene	E	12	174	55	354	35	84	0	0.6	5	14
							S	7	349	6	239	74	80	15	0.52	16	49
							C	6	72	4	337	45	166	44	0.55	3	28
BRIGAND	10.497367	-61.074050	710831	1161088	Guaracara Mb	Middle Miocene	E	11	341	76	135	13	227	6	0.52	12	39
							S	13	124	30	315	60	216	5	0.45	11	25
BATCHA1	10.369283	-61.342983	681417	1146713	Guaracara Mb	Middle Miocene	S	12	140	2	37	81	231	9	0.36	9	32
BATCHA2	10.372300	-61.343500	681358	1147049	Guaracara Mb	Middle Miocene	E	6	284	70	114	20	23	3	0.22	16	36
							S	18	137	17	244	43	31	42	0.02	8	46
							S	19	261	1	354	67	171	23	0.38	7	22
MAYO1	10.360000	-61.370000	678143	1145604	Guaracara Mb	Middle Miocene	S	25	243	26	45	63	150	7	0.45	11	36
							S	10	175	20	44	60	273	21	0.4	9	31
							S	7	123	7	335	82	213	4	0.32	15	58
MAYO2	10.359033	-61.367450	678743	1145567	Guaracara Mb	Middle Miocene	S	17	130	15	333	74	222	6	0.33	10	43
							E	5	315	66	112	22	206	8	0.24	16	36
BICHE	10.423567	-61.147916	702745	1152837	Guaracara Mb	Middle Miocene	S	23	166	8	359	82	256	2	0.54	11	25
							S	6	76	8	330	63	170	26	0.51	11	31
GASPARI	10.333067	-61.425717	672378	1142663	Pointe a Pierre	Paleocene-Eocene	E	14	86	31	291	56	183	12	0.356	15	31
							C	13	279	19	188	4	86	71	0.23	13	38
FERNANDO	10.281633	-61.458210	668845	1136883	Naparima Hill	Cretaceous	SC	10	357	25	210	61	93	14	0.3	10	32

|

|